The dynamics of liquid hydrogen and liquid nitrogen studied by inelastic neutron scattering

da Costa Carneiro, Kim

Publication date:
1974

Document Version
Publisher's PDF, also known as Version of record

Risø Report No. 308

Risø Report No. 308

Danish Atomic Energy Commission

Research Establishment Risø

The Dynamics of Liquid Hydrogen and Liquid Nitrogen Studied by Inelastic Neutron Scattering

by Kim da Costa Carneiro

May 1974

Sales distributors: Jul. Gjellerup, 87, Sølvgade, DK-1307 Copenhagen K, Denmark

Available on exchange from: Library, Danish Atomic Energy Commission, Risø, DK-4000 Roskilde, Denmark

May 1974 Risø Report No. 308

The Dynamics of Liquid Hydrogen and Liquid Nitrogen Studied by Inelastic Neutron Scattering *

by

Kim da Costa Carneiro

Danish Atomic Energy Commission
Research Establishment Risø
Physics Department

Abstract

Recent experimental studies of liquids have shown that phonon-like collective excitations seem to exist in some liquids but not in others. Consequently the assumption for the ideal phonon theory used to describe lattice dynamics is analysed, and non-crystalline materials are classified according to which assumptions are obeyed and which are violated. The neutron scattering results from liquid H_2 are critically analysed with the result that the concept of phonons must be introduced to understand this liquid, and consequently the phonons are quantitatively discussed. In liquid N_2 no evidence of phonons is seen in the neutron scattering pattern, in agreement with the results obtained for liquid A. The influence of the rotational degrees of freedom in liquid N_2 is briefly discussed. The results presented together with similar results obtained from the liquids A, He, and Rb support the classification mentioned above, and indicate how further understanding of the dynamics of liquids may be gained. In an appendix the use of a neutron triple axis crystal spectrometer in the study of liquids is discussed.

* This report is submitted to the University of Copenhagen in partial fulfilment of the requirements for obtaining the Ph. D. degree.

UDC 546.11-14 + 546.17-14 : 539.2 : 539.171.4

ISBN 87 550 0269 2

CONTENTS

Page

1. INTRODUCTION

Until a few years ago it was generally believed that the high frequency, low wavelength dynamics of liquids were similar to phonons in crystals. The experimental evidence supporting this was the observation of well defined collective excitations in superfluid liquid ^{4}He[1] and further the similarity between raw neutron time of flight data obtained from liquids and from solids[2-3].

The last two years have brought two kinds of experimental information proving that the concept of phonons does not apply to liquids in general. Neutron Scattering (NS) data presented as normalized scattering laws (the Fourier transforms of the van Hove correlation functions), and Molecular Dynamics (MD) computer simulation on classical fluids with a given interaction potential, have shown that the existence of well-defined collective excitations depends critically on which system is under study. Phonon-like excitations have been reported in liquid ^{4}He[4], liquid H_2[5], and liquid Rb[6-7], whereas in classical Lennard-Jones liquids[8-9] one cannot in any consistent way introduce the concept of phonons for the collective excitations, which here seem to be of an overdamped nature.

The theoretical attempts to explain the observed phenomena have so far been rather few and unable to reveal the underlying physical concepts. Although partial agreement between theories based on memory functions and the experiments have been found in the case of classical Lennard Jones liquids[10], these theories have been based on the use of sum rules rather than on first principes. Attempts to set up a theory based on first principles suffer from simplifying assumption as this many-body problem does not in a natural way reduce to a dynamical problem for a few quasi-particles.

In the long wavelength limit where linear hydrodynamic theory for viscous fluids gives detailed agreement with the results of light scattering, complete understanding of the dynamical behaviour exists, but since this region cannot be reached by NS, it will not be covered here. However MD results at wavevectors $0.2\ \text{Å}^{-1} < \kappa < 1\ \text{Å}^{-1}$ for liquid A[9] may be understood by introducing a coupling between longitudinal and transverse modes. This wavevector range should be studied in detail by NS in the near future, and a first attempt of this kind is presented in chapter 4.

Apart from this point the discussion will be restricted to wavevector and energy regions so far explored by neutron scattering. Further, since the motion of the only molecular centres in solids are described by phonons, the discussion will be restricted to cases where this motion can be studied

solely and unambiguously in the liquid phase. Finally the dynamics of the superfluid phase will be omitted, since the existence of the superfluid condensate does not in a simple way allow relation of the dynamics of this phase to normal (i. e. not superfluid) liquids. Because of the similarity of the superfluid transition to solidifying, the lambda point will in the discussion be analoguous to the triple point, and all liquids discussed in this report were then studied close to their triple point.

The purpose of this report is to discuss the dynamical behaviour of the non-crystalline phases as compared with phonons in crystals. Considering the theoretical situation described above even a rough classification of liquids from the point of wiew of their dynamical properties may be of interest. This is tried in chapter 2, where the assumptions obeyed in ideal phonon theory break down in different ways for the different classes. For completeness a brief discussion of the dynamical behaviour of non-crystalline solids and supercooled liquids will be given.

In chapters 3 and 4 the dynamics of liquid H_2 and N_2 are discussed. In each case the neutron scattering properties are explained and the discussion is divided into three parts: First a brief discussion will be given of what conclusions can be drawn from the structure factor $S(\varkappa)$, which is the Fourier transform of the static pair correlation function g(r). Secondly the collective motion are discussed based on the coherent scattering law $S_{COH}(\varkappa,\omega)$, which is the Fourier transform of the total van Hove correlation function G(r, t). Thirdly the single particle motion are discussed based on the incoherent scattering law $S_{INC}(\varkappa,\omega)$, related to the van Hove selfcorrelation function $G_s(r, t)$.

On the basis of the classification of chapter 2 chapter 5 gives a conclusion about how the dynamical behaviour of liquids may conceptually be understood. Further possible future research is discussed.

In an appendix the use of a triple axis spectrometer in the study of liquids is discussed and compared with the time of flight spectrometer.

2. DYNAMICAL BEHAVIOUR OF NON-CRYSTALLINE MATERIALS

When atoms or molecules are ordered in lattices the dynamical behaviour can be theoretically understood in terms of phonons. It is instructive to analyse the basic assumptions for this theory in the ideal case, and to see how these assumptions are fulfilled to various degrees for real crystals. However, even where strong deviations from the ideal case make the establishing of a dynamical theory difficult, the resulting excitations

carry many of the characteristics of good phonons. This indicates that in the crystalline phase the existence of phonons is relatively insensitive to the fulfilment of the basic assumptions. After a discussion of these, an attempt will be made to classify liquids according to which assumptions break down, and expected similarities within one class will be pointed out. A brief discussion of the known dynamical behaviour will be given, and it will be shown why studies of liquid H_2 and liquid N_2 are expected to give useful information.

2.1. Ideal and Real Crystalline Solids

Four assumptions may be considered of basic importance for establishing the theoretical picture of phonons in ideal crystals. The first to be mentioned is the assumption of a perfect periodic structure. This allows a division of the dynamical problem for all the atoms in the crystal into independent sets of dynamical problems for 3n phonons, where n is the number of atoms in the unit cell. For liquids MD[9] results show that the dynamical behaviour is well described with a unit cell of 500-1000 atoms. This number does not at present allow the dynamical matrix to be solved, although it indicates that the problem of how the lack of periodicity influences the dynamical behaviour is numerical in nature rather than conceptual.

A second assumption is that the system is stationary. More general, the phonons have to be the only excitations of the system, but in liquids in particular the single particle diffusion is known to be present. If the single particle diffusion occurs at a time scale much larger than the phonons, one expects from energetic considerations both excitations to remain well defined. However, if this is not the case, i. e. if the self diffusion and the possible phonons occur at similar time scales, the question to be answered is whether each of the two different kinds of motion retains its simple character in the presence of the other, or whether a mutual coupling destroys both.

Thirdly, in setting up the exact theory for phonons, one assumes the temperature to be zero. At finite temperatures, thermal population introduces phonon-phonon interactions if the interaction potential is not strictly harmonic. The weak anharmonicity present in any crystal does, however not manifest itself provided the temperature T is low compared with the Debye temperature θ_D of the solid. Consequently T/θ_D will be used as a convenient measure of the "dynamical" temperature. At higher temperatures pertubation theory accounts well for the observed changes of the

phonons, so that the assumption of low temperatures can be abandoned in the crystalline case without losing understanding of the system.

Closely related to this assumption is the fourth to be mentioned, the assumption of a harmonic interacting potential. When critical phenomena are not considered, anharmonic effects, however, cause rather small changes in the phonon spectra, compared to the ideal case. Even in the case of quantum crystals (^{4}He, H_2, and D_2)[11-12], where the particle positions have to be changed into single particle wavefunctions, the strong effective anharmonicity hereby introduced still allows the phonons to be good quasi-particles.

As appears from the above, in real crystals either the assumptions for the ideal phonon theory are obeyed or deviations can be treated as perturbations. This is not the case in liquids. In general all four assumptions cease to be valid, and since no first principles' theory has been established, very little is at present known about the specific influence on the dynamical behaviour in the liquid phase from each of the four basic assumptions mentioned. It is therefore interesting that non-crystalline materials can be classified according to what assumptions are violated. This is shown in table 1, and in the following a discussion of the classes hereby defined is given. As a reference the "ideal crystalline solids" are shown in the first column, and the second column corresponds to the discussion of real crystals.

Table 1

Possible classification of non-crystalline materials relevant for their dynamical properties. The assumptions are fulfilled in the exact theory for phonons but are violated differently by the different classes. D = "dependent" means that the assumption may be obeyed for some systems in the class and not for others

	SOLIDS			LIQUIDS			
Assumption	Ideal crystalline	Real crystalline	Amorphous	Super-cooled	Quantum	Metallic	Lennard-Jones
Periodicity	Yes	Yes	No	No	No	No	No
Stationarity	Yes	Yes	Yes	D	No	No	No
Low Temperature	Yes	D	D	D	Yes	No	No
Harmonic Potential	Yes	D	D	D	No	Yes	No

2.2. Amorphous Solids

The third column in table 1 shows the amorphous solids only deviating from the crystalline solids in being disordered. Since the lack of periodicity is present in all classes, it is of interest that this effect appears isolated. Both from theoretical and experimental evidence it is now clear that the dynamical behaviour of non-crystalline solids differs significantly from that of the corresponding crystal. Kim and Nelkin[13] have in one dimension theoretically compared the harmonic solid in the ordered and the disordered phase. They found a rather small shift in the phonon frequencies, but in addition a finite linewidth in the disordered state. Although phonon line shapes have not been measured by NS for glasses, two sets of experiments strongly support the results of Kim and Nelkin. The specific heat in glasses at low temperatures[14] exceeds the Debye-specific heat found in crystals. Although several models have been proposed to explain this frequent anomaly, the most plausible explanation at the moment seems to be a change of the phonon spectrum[15]. Consequently Stephens[14] calculated, on the basis of harmonic oscillators, the density of phonon states $Z(\omega)$ from the measured specific heat. Owing to the excess specific heat a considerable excess density of states at low energies is found, in addition to the density of states prescribed by the Debye model. Recent NS measurements of the phonon density of states in Ge[16] show that at low energies $Z(\omega)$ for the amorphous solid exceeds that of the crystal. Further $Z(\omega)$ does not seem to approach its Debye value for $\omega \to 0$, which it does in the crystalline case.

2.3. Supercooled Liquids

In the fourth column of table 1 the supercooled liquids appear like glasses except for the fact that they may be studied where the single particle diffusion occurs at a time scale gradually approaching that of the collective excitations. Comparison between the dynamical behaviour of glasses and supercooled liquids may therefore serve as a test for the importance of the assumption of stationarity. Except for a few examples such as Ga, which has only been studied by diffraction[19], only rather complicated materials can easily be supercooled. However, Mössbauer effect studies from such materials[18] indicate a correlation between the collective and single particle excitations; but a discussion of whether good phonons exist cannot be given at present.

2.4. Quantum Liquids

The remaining three columns in table 1 contain the normal thermocynamically stable liquids. They are disordered and further the non-stationarity is quantitatively described by the self diffusion coefficient $D = 2 - 6 \times 10^{-5}$ cm^2/s. However, natural abundance provides three classes to be mentioned according to the two last assumptions discussed above. As mentioned in the introduction superfluidity will not be discussed in detail, but one comment will be made. In the superfluid phase of ^{4}He, very phonon-like excitations are known to exist and have been studied extensively[4]. The existence of these excitations has often treated as being closely related to superfluidity, although it is not clear how the superfluid condensate should have a drastic effect on the total short wavelength density fluctuations.

It is therefore not astonishing, although often overlooked that collective excitations exist in the normal phase of liquid ^{4}He[4]. However, this fact introduces the question of whether the normal quantum liquids, (^{4}He, ^{3}He, H_2, D_2, and Ne) because of the low temperatures at which these liquids exist, are in general able to support short-wavelength collective excitations. This problem will be elucidated in chapter 3 where the study of liquid H_2 is presented. This liquid is of interest because it exists at very low temperatures, and further the special neutron scattering properties makes it possible to study both $S_{COH}(\varkappa,\omega)$ and $S_{INC}(\varkappa,\omega)$, providing a stringent test on the possible existence of phonons. Finally it is important that the phonons have been studied in detail in the solid phase[12].

In table 1 the interacting potential is listed as being not harmonic for quantum liquids. The molecules in the quantum liquids are known to interact via a Lennard-Jones potential, and quantum effects seem in the liquid phase to be well described as a temperature effect. This is qualitatively shown in fig. 1. Although the Lennard-Jones potential appears far from harmonic, the low temperature of the quantum liquid may have the consequence that only the lowest states are thermally populated.

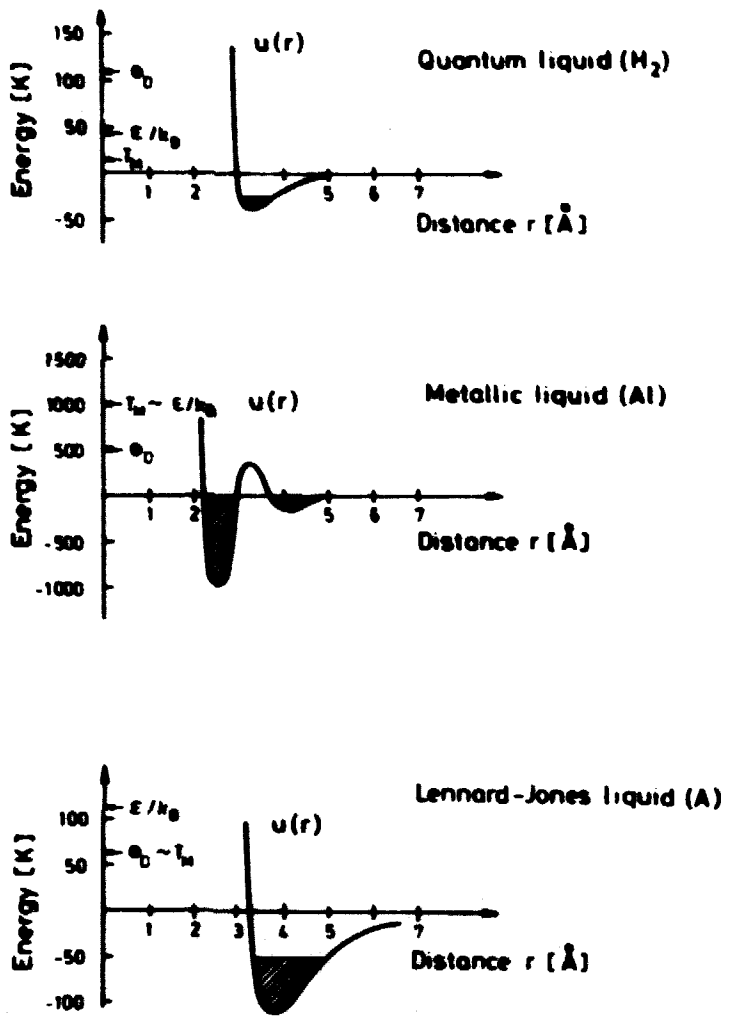

Fig. 1. Characteristic potentials and temperatures in quantum liquids, metallic liquids and Lennard-Jones liquids. ε = well depth of potential, T_M = melting point, and Θ_D = Debye temperature of the solid.

2.5. Metallic Liquids

Contrary to quantum liquids, liquid metals appear at high temperatures with fairly harmonic interaction potentials. As will be seen from fig. 1, the thermal population in the metallic case is considerable, but the form of the potential indicates that the populated states are predominantly harmonic in nature. It is therefore interesting that recent NS[6] and MD[7] results for liquid Rb show that phonons of intermediate wavelengths (i. e. in the wavevector region 0.3 $\mathring{A}^{-1} < \kappa < 1.2\ \mathring{A}^{-1}$), although heavily damped, exist in this liquid.

2.6. Lennard-Jones Liquids

In the last column of table 1 are shown the classical Lennard-Jones liquids. All the four basic assumptions necessary for establishing an exact theory for phonons are violated. Consequently, no consistent evidence for

phonons was found in the extensive NS[8] study of liquid A, neither in $S_{COH}(\kappa,\omega)$ nor in $S_{INC}(\kappa,\omega)$. However, the important question may still be asked, of whether the Lennard-Jones potential, shown for A in fig. 1, is relevant for the understanding of the dynamical properties of these liquids. This question has so far been answered positively in part by comparison between NS[8] and MD[9] results; but an alternative test is to prepare another Lennard-Jones liquid at a state corresponding to that of liquid A, and to see if scaling according to the potential parameters is obeyed. The concept of a state[19] is briefly discussed below.

Liquid N_2 was then studied by NS and the results are presented in chapter 4. The parameters of importance for the scaling[19] are shown in table 2. σ_{LJ} and ϵ_{LJ} are the Lennard-Jones potential parameters used to scale distance and temperature respectively. $\tau_{LJ} = (M\sigma_{LJ}^2/(48\epsilon_{LJ}))^{1/2}$, where M is the molecular mass, is used to scale time. The states may then be described by T^* and ρ^*.

Table 2

Parameters of importance for the scaling via the principle of corresponding states for the liquids A, N_2, H_2, and ^4He. The reduced state parameters T^*, ρ^* correspond to temperatures and densities where neutron scattering has been performed

	σ_{LJ}[Å]	ϵ_{LJ}/k_B[K]	τ_{LJ}[ps]	T^*	ρ^*	Λ^*
A	3.405	119.8	0.312	0.71	0.83	0.19
N_2	3.70	94.9	0.234	0.70	0.93	0.23
H_2	2.93	37.0	0.114	0.39	0.54	1.73
^4He	2.58	10.2	0.287	0.26	0.32	2.68

Further in table 2 is shown the de Boer parameter $\Lambda^* = (h/\sigma_{LJ})(M/\epsilon_{LJ})^{1/2}$. If a state is then defined by T^*, ρ^*, and Λ^*, scaling should be obeyed between all liquids interacting through the Lennard-Jones potential including the quantum liquids[19]. However, since no dynamical theory can at present relate short wavelength dynamical properties from one state to another, only different systems such as N_2 and A, prepared in the same state can be compared. The quantum nature of a liquid, quantitatively defined by the magnitude of Λ^* does not allow a detailed comparison between liquids with

small and large Λ^*. This justifies the fact that the quantum liquids in table 1 are classified separately according to the low temperature at which they exist.

3. NEUTRON SCATTERING IN LIQUID H_2 AT 14.7 K

In the previous chapter liquids were classified according to their expected dynamical properties. It was mentioned that liquid H_2 was a good candidate for testing whether phonon-like collective excitations exist in a low-temperature, anharmonic liquid. In this chapter the results of NS in this liquid will be discussed. The results for the collective excitations have been published[5], whereas a more detailed presentation will be published for the single-particle motion[20]. Here the results will be reviewed and compared with the results for liquid A, and when possible also with liquid ^4He.

3.1. Neutron Scattering Properties of Molecular Hydrogen

Molecular hydrogen has very special neutron scattering properties. This is due to the existence of the para and ortho modifications p-H_2 and o-H_2. In fig. 2 is shown how the symmetry of the molecular wavefunction Ψ divides the rotational states into two groups, the para states where the rotational quantum number J is even and the total spin I=0, and the ortho states where J is odd and I=1. Because of the small moment of inertia of the H_2 molecule and because the anisotropic interactions are small, J is

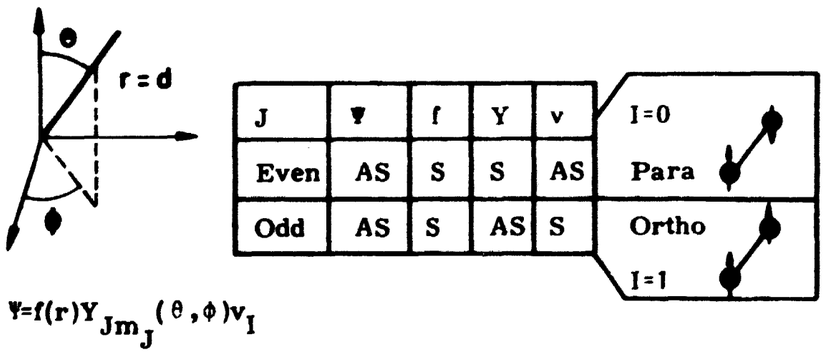

Fig. 2. Symmetries of the molecular wavefunction Ψ, in the case of H_2, when the two protons are interchanged. S = symmetric, AS = antisymmetric. At the right are shown the resulting spins of the protons corresponding to the symmetry of the spin function v_I.

a good quantum number. Further, since the energy of the first rotational state $\Delta E = E_{(J=1)} - E_{(J=0)} = 14.6$ meV = 170 K, only p-H_2 with J=0 and o-H_2 with J=1 are present below the boiling point $T_B = 20.4$ K. One important consequence of fig. 2 is that p-H_2 has I=0 i.e. a spin singlet eigenstate. This makes the neutron scattering within the J=0 state purely coherent, so that p-H_2 acts as a scatterer with a coherent scattering length per molecule of $2 \cdot b_{coh} \cdot j_0(\varkappa d/2)$. b_{coh} is the coherent scattering length for the proton, d=0.746 Å is the internuclear bond length, and j_0 is the zero order spherical Bessel function. $\varkappa$ is the wavevector transferred to the liquid by a neutron.

Sarma[21] has worked out the full expressions for the neutron scattering from all the combinations of p-H_2 and o-H_2. The scattering cross sections for neutrons that do not undergo energy changes large enough to change the rotational state are:

<u>1: (J=0) → (J=0) scattering:</u>

$$\frac{d^2\sigma}{d\Omega d\omega} = c_0 \frac{k}{k_0} \frac{h}{\pi} \sigma_{COH} j_0^2 (\tfrac{\varkappa d}{2}) S_{COH}(\underline{\varkappa}, \omega) \qquad (1)$$

where

$$S_{COH}(\underline{\varkappa}, \omega) = \frac{1}{2\pi\hbar} \int_{-\infty}^{\infty} dt \int d\underline{r}\ e^{i(\underline{\varkappa} \cdot \underline{r} - \omega t)} G(\underline{r}, t) ,$$

<u>2: (J=1) → (J=1) scattering:</u>

$$\frac{d^2\sigma}{d\Omega d\omega} = c_1 \frac{k}{k_0} \frac{h}{\pi} (\sigma_{COH} + \frac{2}{3} \sigma_{INC}) \{ j_0^2(\tfrac{\varkappa d}{2}) + 2 j_2^2 (\tfrac{\varkappa d}{2}) \} S_{INC}(\underline{\varkappa}, \omega) \qquad (2)$$

where

$$S_{INC}(\underline{\varkappa}, \omega) = \frac{1}{2\pi\hbar} \int_{-\infty}^{\infty} dt \int d\underline{r}\ e^{i(\underline{\varkappa} \cdot \underline{r} - \omega t)} G_s(\underline{r}, t) .$$

If we, however, make the neutron energy large enough to excite the para-ortho transition, the cross-section is:

<u>3: (J=0) → (J=1) scattering:</u>

$$\frac{d^2\sigma}{d\Omega d\omega} = c_0 \frac{k}{k_0} \frac{h}{\pi} 3\sigma_{INC} j_1^2 (\tfrac{\varkappa d}{2}) S_{INC}(\underline{\varkappa}, \omega - \tfrac{\Delta E}{\hbar}) . \qquad (3)$$

In (1)-(3) $G(\underline{r}, t)$ and $G_s(\underline{r}, t)$ are the total and self-correlation functions for the molecular centres, respectively. $\underline{k}_0$ and $\underline{k}$ are the incoming and outgoing wavevectors of the neutrons, $\hbar\underline{\varkappa} = \hbar(\underline{k}_0 - \underline{k})$ and $\hbar\omega = \hbar^2(k_0^2 - k^2)/(2m)$ are the momentum and energy transferred to the liquid by one neutron. $\sigma_{COH} = 1.77$ barns and $\sigma_{INC} = 79.9$ barns are the nuclear coherent and incoherent scattering cross sections respectively.

Two simplifying cases occur if either the ortho concentration c_1 or the para concentration c_0 becomes unity, and the results are summarized in fig. 3. In pure $o\text{-}H_2$, studied by Egelstaff et al.[22], only scattering according to (2) occurs, giving the incoherent scattering law $S_{INC}(\varkappa, \omega)$.

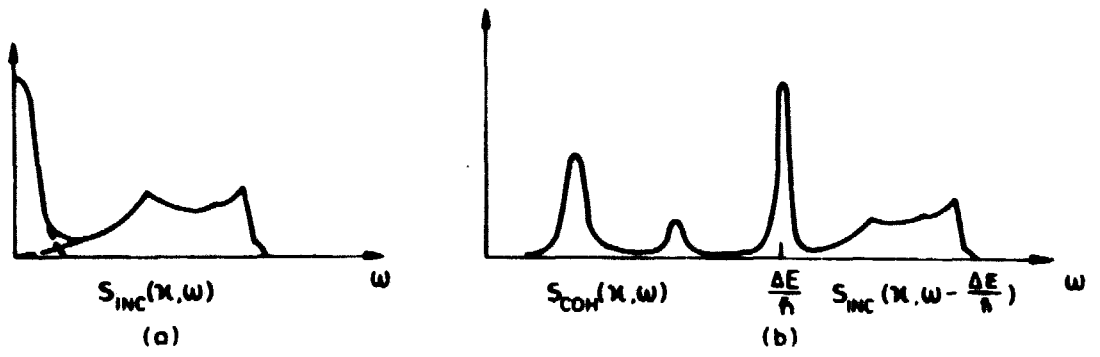

Fig. 3. Neutron scattering from molecular hydrogen obtained by a constant wavevector experiment.

(a) Scattering from $o\text{-}H_2$ yielding $S_{INC}(\varkappa,\omega)$.

(b) Scattering from $p\text{-}H_2$ yielding $S_{COH}(\varkappa,\omega)$ and $S_{INC}(\varkappa,\omega)$.

In pure $p\text{-}H_2$ studied here, scattering according to (1) and (3) occurs. Since the total width of the coherent spectrum is observed to be 8 meV, (1) and (3) show that it is effectively separated from the incoherent spectrum by the translation in energy ΔE. In the coherent scattering experiment the neutron energy is therefore made smaller than 14.6 meV, so that only scattering according to (1) is possible. For higher incoming energies the scattering is dominated by the incoherent process (3) when $\Delta E < \hbar\omega < 2\Delta E$. This is true even if $S_{COH}(\varkappa, \omega)$ differs from zero in this range, because of the large ratio $\sigma_{INC}/\sigma_{COH}$. In fig. 3 the scattering laws are shown essentially one-sided. This is a good approximation because of the principle of detailed balance:

$$S(\varkappa, -\omega) = e^{-\hbar\omega/k_B T} S(\varkappa, \omega), \qquad (4)$$

which together with the energy shift ΔE provides the separation of the scattering laws.

Equations 1 and 3 therefore allow the determination of both S_{COH} and

S_{INC}, and data were obtained using a triple axis neutron spectrometer. The instrumental corrections were performed according to the procedure discussed in the Appendix. The only point where the interpretation of the data differs from the simple monoatomic case, is the appearance of the molecular form factors j_0^2 and j_1^2. These functions are shown in fig. 4.

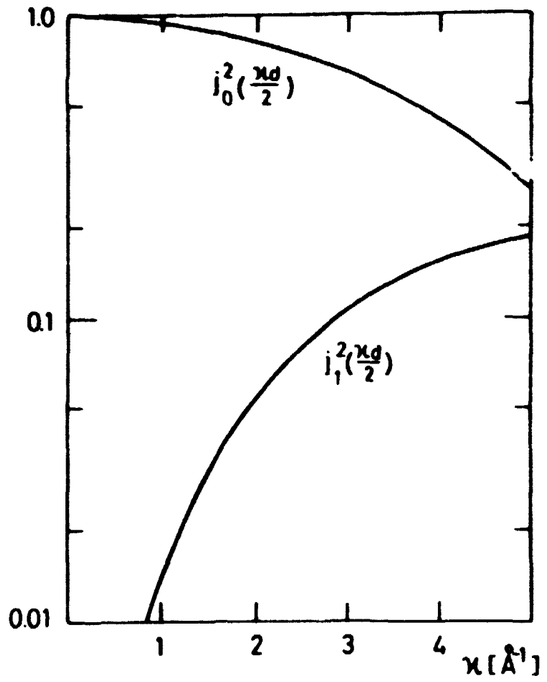

Fig. 4. Formfactors of interest for the interpretation of the cross sections for molecular H_2.

Finally it should be mentioned that in practice the concentrations c_0 and c_1 play an important role for the success of an experiment. The equilibrium value at T_B for c_1 is 0.2%, so that even the slow decay towards equilibrium changes c_1 from its initial room temperature value of 75% during a neutron scattering experiment on predominantly o-H_2. If almost pure p-H_2 is studied, even a small inefficiency in the catalyzation process to reduce c_1 immediately introduces a complicated scattering pattern with both coherent and incoherent scattering according to (1) and (2).

3.2. Experimental Results for Liquid H_2 at 14.7 K

3.2.1. The Structure Factor

Although the liquid structure factor $S(\varkappa)$ is not directly dynamical in nature, it is usual to start the presentation of the neutron scattering results

by showing $S(\varkappa)$. This is done for the liquids A[8], H_2, and ^{4}He[23] in fig. 5.

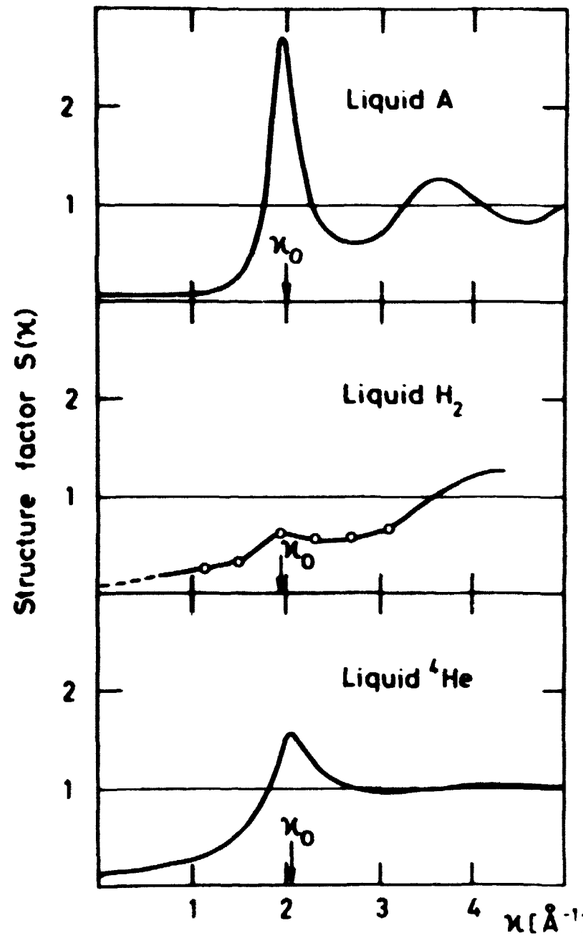

Fig. 5. Structure factor $S(\varkappa)$ for the three liquids A, H_2, and ^{4}He.

The peculiar shape of $S(\varkappa)$ for H_2 was verified through both a diffraction experiment and the relation:

$$S(\varkappa) = \int_{-\infty}^{\infty} S_{COH}(\varkappa, \omega)\, d\omega \,. \qquad (5)$$

Fig. 5 shows that the structure factor does not scale in a simple way according to σ_{LJ}, shown in table 2, but indicates that a complicated function of all three state parameters must be used to describe the structure at different states. This picture is somewhat simplified when $S_{COH}(\varkappa, 0)$ is studied at the end of the next section.

3.2.2. Collective Motion

The obtained $S_{COH}(\varkappa,\omega)$ is presented in fig. 6 for the wavevector values $\varkappa$ = 0.7, 1.1, 1.5, 1.9, 2.3, 2.7, and 3.1 Å^{-1}. $S_{COH}(\varkappa,\omega)$ has been normalized through the ACB sum rule described below. For small $\varkappa$'s momentum conservation limits the accessible range of ω in $S_{COH}(\varkappa,\omega)$ for a given energy of the incoming neutrons, which was kept below 14.6 meV. In liquid hydrogen this means that one cannot at the present temperature measure the longitudinal phonon branch for $\varkappa \geq 1.0$ Å^{-1} because of the high sound velocity.

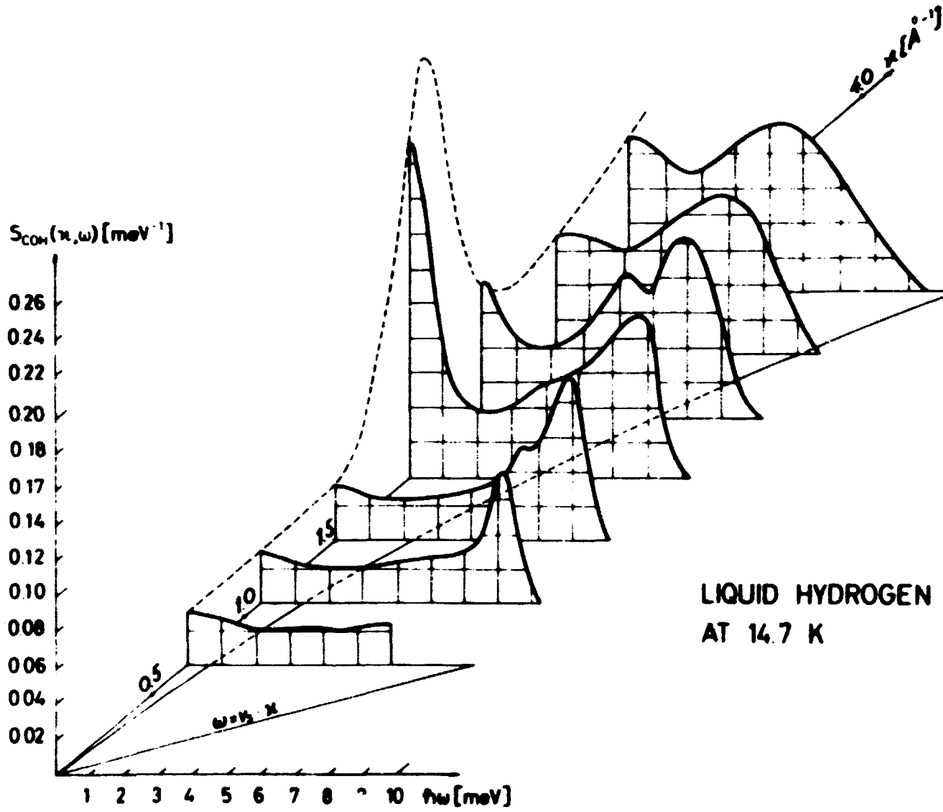

Fig. 6. Coherent scattering law $S_{COH}(\varkappa,\omega)$ for liquid parahydrogen at T = 14.7 K and saturated vapour pressure. In the base plane the recoil energy curve is shown, and the extension of the position of the Brillouin peak is indicated.

Fig. 6 demonstrates that a well-defined peak exists in $S_{COH}(\varkappa,\omega)$ for $\omega \neq 0$, signifying the existence of a collective excitation in the density-density correlation function. In liquid A such peaks are not seen in $S_{COH}(\varkappa,\omega)$, but only in the velocity autocorrelation function $\omega^2 S(\varkappa,\omega)$, which of course has a peak at finite energy even if the density-density correlation function is overdamped. In addition to the maximum at finite frequency in liquid H_2 there is also a portion of the spectrum centred at zero frequency, most pronounced at $\varkappa$ = 2 Å^{-1}, i.e. near the "major" peak in the structure factor. In this respect liquid H_2 is similar to classical liquids.

Compared with liquid ^{4}He above the λ point[4] liquid H_2 is similar in the sense that both liquids seem to support well-defined propagating modes, but in ^{4}He no elastic line occurs. This may reflect the fact that the specific heat ratio C_p/C_v is close to unity, which in the hydrodynamic region would make the central Rayleigh line disappear.

After it has been shown that in the quantum liquids the significant inelastic part of $S_{COH}(\varkappa,\omega)$ indicates the existence of phonons, two rigorous tests will be made. The first is to compare $S_{COH}(\varkappa,\omega)$ with that expected from polycrystalline H_2. For instance the energy of the longitudinal phonon at the first zone boundary in the solid is 10 meV at $\varkappa$ = 1.0 Å^{-1}. Estimation from the Gruneisen relation:

$$\gamma = \frac{d(\ln\omega)}{d(\ln\rho)}, \qquad (6)$$

where γ is taken from ref. 12, and ρ is the density, gives 7.5 meV at $\varkappa \simeq 1.0$ Å^{-1} in the liquid. This compares favourably with the peak observed in $S_{COH}(\varkappa,\omega)$ at 7.2 meV.

At higher $\varkappa$'s, corresponding to the second and third Brillouin zones in the solid, intensity appears in the liquid at lower energy, resembling of the neutron scattering law calculated for a polycrystalline powder. In the latter case this additional feature is related to modes which have an appreciable transverse character, suggesting that transverse modes may contribute to the scattering in the liquid, although it is not clear how the neutron can couple to transverse modes in the absence of a reciprocal lattice. Such a coupling would imply that the liquid as a whole, similar to a crystal lattice, could take up momentum of $\hbar\varkappa_o$, where $\varkappa_o$ is the wavevector at which the first peak in the structure factor occurs. In our case $\varkappa_o$ = 2 Å^{-1}, which is close to an average of the first three Bragg peaks in the solid.

The second test is the ACB (Ambegaokar, Conway and Baym) one-phonon sum rule[25] which is a specialization of the universal Placzek sum rule. The Placzek sum rule states that:

$$I_p = \int_{-\infty}^{\infty} d\omega \omega S_{COH}(\varkappa, \omega) = \varkappa^2/(2M) \qquad (7a)$$

Applying (4), (7a) becomes:

$$I_p = \int_{0}^{\infty} d\omega (1 - \exp(-\hbar\omega/k_B T)) \omega S_{COH}(\varkappa, \omega) = \varkappa^2/(2M) \qquad (7b)$$

For a cubic, harmonic solid the ACB sum rule then states that the one-phonon part S_{COH}^{PH} of S_{COH} obeys the relation similar to (7):

$$I_{ACB} = \int_{0}^{\infty} d\omega (1 - \exp(\hbar\omega/k_B T)) \omega S_{COH}^{PH}(\varkappa, \omega) = \frac{\varkappa^2}{2M} \exp(-\tfrac{1}{3}\varkappa^2 \langle u^2 \rangle). \qquad (8)$$

In fig. 7 we show $I_{ACB}(2M/\varkappa^2)$ obtained from the spectra shown in fig. 6. The fact that the spectra agree well with a mean square displacement, is a strong indication that the measured portion of $S_{COH}(\varkappa, \omega)$ in

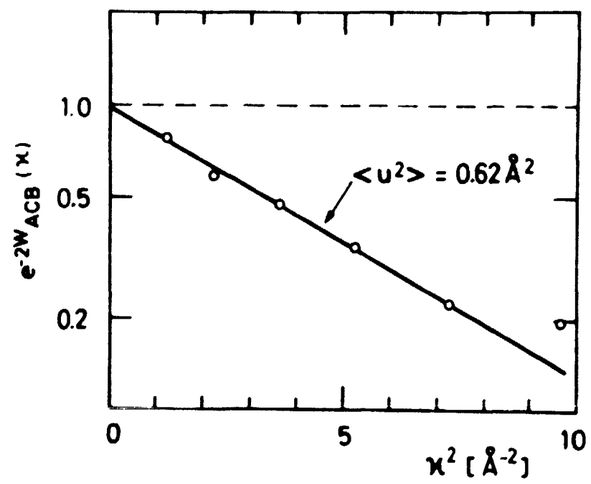

Fig. 7. The ACB one-phonon sum rule applied to the measured spectra. The dashed line corresponds to the Placzek sum rule for the total scattering. The finite slope of the solid line through the measured points corresponds to a mean square displacement $\langle u^2 \rangle = 0.62$ Å^2.

liquid H_2 consists of phonon contribution. Consequently (8) was used to normalize S_{COH} and the value of $\langle u^2 \rangle$ was found to be 0.62 Å^2 [x]. In liquid A the spectra obeyed eq. (7) and no natural division of the spectra could be made.

At this point the following conclusion can be drawn about the collective excitations in liquid H_2. They are qualitatively well described by phonons. From their "zone boundary value" and the sum rule the phonons are quantitatively defined by the Debye temperature θ_D - 70 K and the mean square displacement $\langle u^2 \rangle = 0.62$ Å^2. The corresponding values in the solid phase[12] are $\theta_D = 102$ K and $\langle u^2 \rangle = 0.48$ Å^2. In ^{4}He, θ_D may be taken to be 15 K in the liquid phase compared with 25 K in the solid, whereas in liquid A, θ_D and $\langle u^2 \rangle$ cannot be defined from $S_{COH}(\varkappa, \omega)$.

Since considerable interest has been devoted to the function $S_{COH}(\varkappa, 0)$, this function is compared for liquid A[8] and H_2 in fig. 8. Whereas $S(\varkappa)$ is

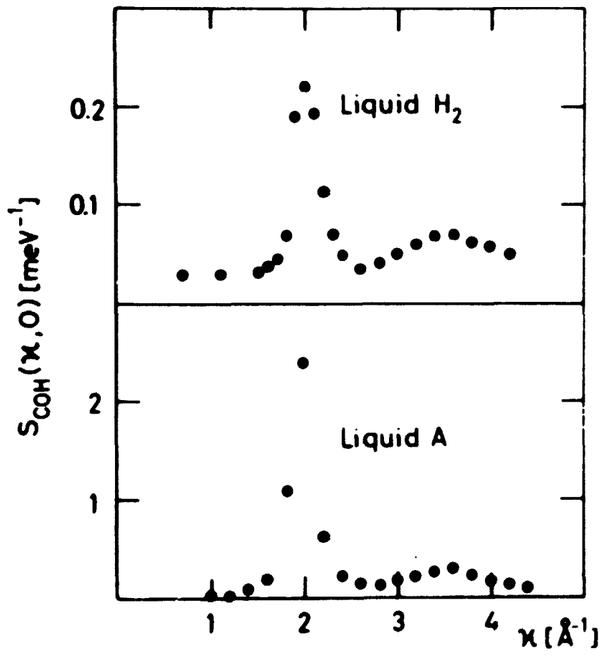

Fig. 8. Comparison of $S_{COH}(\varkappa, 0)$ for the two liquids A and H_2.

[x] The previously reported value $\langle u^2 \rangle = 1.0$ Å^2 in refs. 5, 26, and 27 was due to misinterpretation of the data.

the spatial Fourier transform of G(r, 0), i. e. corresponds to a "snapshot" of the liquid, it appears from eq. 1 that $S_{COH}(\varkappa, \omega)$ corresponds to the time average of G(r, t). The qualitative similarity between the two curves in fig. 8 indicates that the latter is more universal for liquids than the former, shown in section 3. 2. 1.

3. 2. 3. Single Particle Motion

In fig. 9 the incoherent scattering law $S_{INC}(\varkappa, \omega)$ for liquid H_2 is shown for wavevectors $\varkappa$ = 1. 4, 2. 0, 2. 6, and 3. 2 Å^{-1}. $S_{INC}(\varkappa, \omega)$ has been

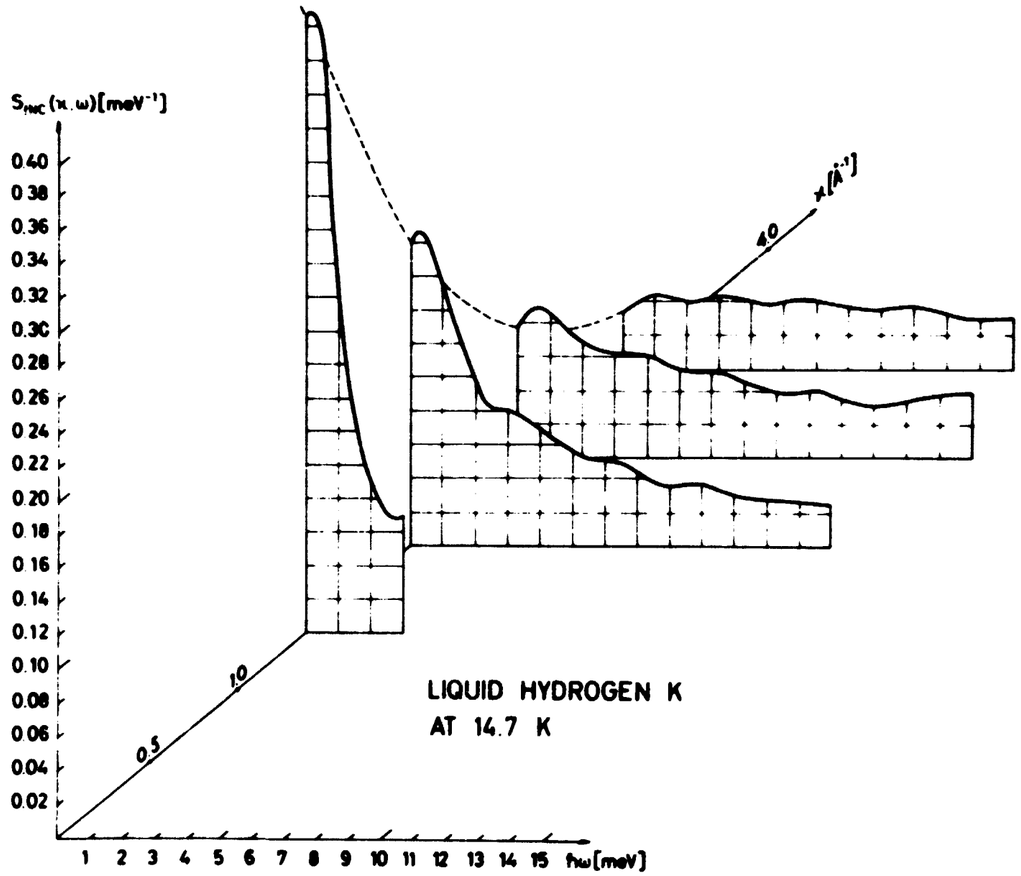

Fig. 9. Incoherent scattering law $S_{INC}(\varkappa, \omega)$ for liquid H_2 at 14. 7 K and saturated vapour pressure.

normalized through the sum rule similar to equation 5:

$$1 = \int_{-\infty}^{\infty} S_{INC}(\varkappa, \omega)\, d\omega \qquad (9)$$

As in the coherent case, experimental constraints limit the accessible range of ($\varkappa$, ω). In agreement with fig. 6 fig. 9 shows considerable inelastic scattering, and in addition an asymmetric central line. In liquid A only the central line could be distinguished.

In the coherent case no theoretical model for the scattering law can be used, but for $S_{INC}(\varkappa,\omega)$ two conceptually different models can be quantitatively discussed. If the single particle motions were due to self diffusion only, the result would be:

$$S_{INC}(\varkappa, \omega) = \frac{1}{\pi} \frac{D\varkappa^2}{(D\varkappa^2)^2 + \omega^2} e^{\hbar\omega/(2k_BT)}, \qquad (10)$$

where D is the self diffusion coefficient. Although several more sophisticated models have been proposed[28], only (10) will be discussed here. It contains the expression for "simple diffusion", but as appears from fig. 9, S_{INC} is not symmetric. Consequently the exponential $e^{\hbar\omega/(2k_BT)}$ is introduced in eq. 10. As proposed by Schofield[29] this correction, closely related to the principle of detailed balance shown in eq. 4, may be used as a first order quantum correction to relate the result of a classical calculation to an observed scattering law.

If on the other hand the individual particles take part, both in diffusion (D) and in phonon-like oscillations (PH) the incoherent scattering law consists of two parts due to the different kinds of motion:

$$S_{INC}(\varkappa, \omega) = S^{D}_{INC}(\varkappa, \omega) + D^{PH}_{INC}(\varkappa, \omega), \qquad (11a)$$

where

$$S^{D}_{INC}(\varkappa, \omega) = \frac{1}{\pi} \frac{D\varkappa^2}{(D\varkappa^2)^2 + \omega^2} e^{\hbar\omega/(2k_BT)} e^{-2W(\varkappa)} \qquad (11b)$$

and

$$S^{PH}_{INC}(\varkappa, \omega) = \frac{\hbar\varkappa^2}{2M} e^{-2W(\varkappa)} \frac{Z(\omega)}{\omega} \frac{1}{1 - e^{-\hbar\omega/(k_BT)}} \qquad (11c)$$

In (11b) the simple diffusion result is modified as discussed in ref. 28 by introducing a Debye Waller factor, and eq. 11c shows the result for one-phonon scattering, where $Z(\omega)$ is the phonon density of states[30].

In the following the measured $S_{INC}(\varkappa,\omega)$ for liquid H_2 will be analysed according to the two possible interpretations, and the results will be compared with similar results for liquid A.

The usual way to analyse incoherent scattering laws is to measure the full width at half maximum (FWHM) of S_{INC} as a function of $\varkappa$. According to simple diffusion

$$\text{FWHM} = 2D\varkappa^2 , \tag{12}$$

which in the case of liquid H_2 is most conveniently analysed using the "symmetrized scattering law":

$$\tilde{S}_{INC}(\varkappa, \omega) = S_{INC}(\varkappa, \omega)\, e^{-\hbar\omega/(2k_BT)} \tag{13}$$

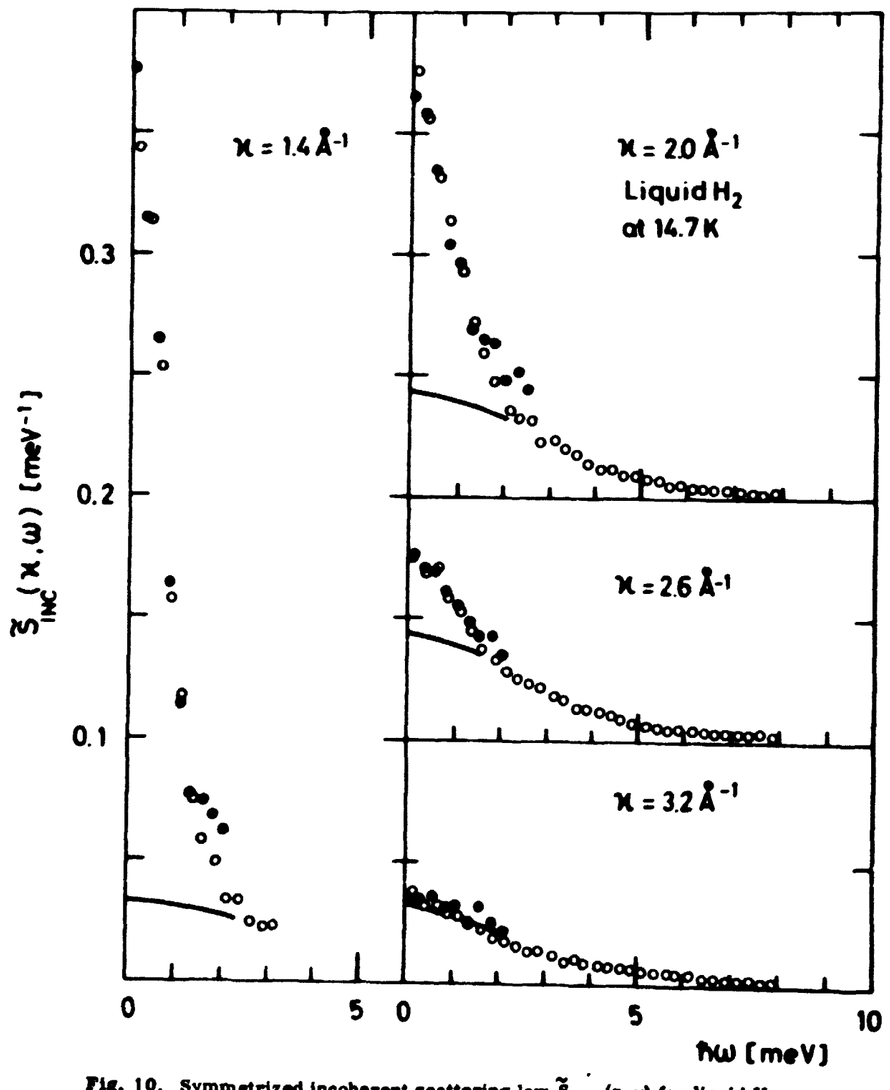

Fig. 10. Symmetrized incoherent scattering law $\tilde{S}_{INC}(\varkappa, \omega)$ for liquid H_2. The solid line corresponds to $\tilde{S}^{PH}_{INC}(\varkappa, \omega)$ as discussed in the text.

This function is therefore shown in fig. 10. According to the two interpretations presented above, we then get from eq. 10:

$$\tilde{S}_{INC}(\varkappa, \omega) = \frac{1}{\pi} \frac{D\varkappa^2}{(D\varkappa^2)^2 + \omega^2} \tag{14}$$

or from eqs. 11:

$$\tilde{S}_{INC}(\varkappa, \omega) = \tilde{S}^{D}_{INC}(\varkappa, \omega) + \tilde{S}^{PH}_{INC}(\varkappa, \omega) \tag{15a}$$

where

$$\tilde{S}^{D}_{INC}(\varkappa, \omega) = \frac{1}{\pi} \frac{D\varkappa^2}{(D\varkappa^2)^2 + \omega^2}\, e^{-2W(\varkappa)} \tag{15b}$$

and

$$\tilde{S}^{PH}_{INC}(\varkappa, \omega) = \frac{\hbar^2\varkappa^2}{2M}\, e^{-2W(\varkappa)}\, \frac{Z(\omega)k_BT}{(\hbar\omega)^2}\, \frac{\hbar\omega/(2k_BT)}{\sinh(\hbar\omega/2k_BT)} \tag{15c}$$

In fig. 11 the FWHM has been determined from eqs. 14 and 15b. In order to substract S^{PH}_{INC}, values for the Debye-Waller factor were taken

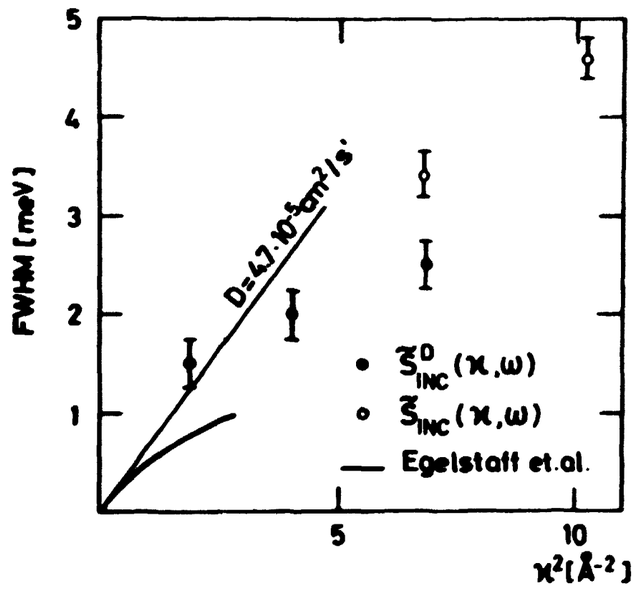

Fig. 11. FWHM of the symmetrized incoherent scattering law $\tilde{S}_{INC}(\varkappa, \omega)$ for liquid H_2 analysed according to the two interpretations discussed in the text.

from the coherent data together with the Debye energy $\hbar\omega_D = k\theta_D$ determining the Debye density of states $Z_D(\omega) = 3\omega^2/\omega_D^3$ for small ω's. Also shown in fig. 11 are the results of Egelstaff et al.[22] together with the results from eq. 12 of simple diffusion, with the diffusion coefficient $D = 4.7 \cdot 10^{-5}$ cm^2/s, as determined from their data. Although there is significant disagreement between the data of ref. 22 and the ones reported here concerning the FWHM, the resulting D agrees fairly well independently of the way the data are interpreted. Consequently the quoted value for D will be used in the following. It is worth noting that in liquid A, significant disagreement with eq. 12 was also found.

In liquid A however, perfect agreement with eqs. 10 and 14 for $\omega = 0$ was found, i.e.:

$$S_{INC}(\varkappa, 0) = \frac{1}{\pi D \varkappa^2} \quad . \tag{16}$$

The alternative interpretation according to eqs. 11 and 15 yields:

$$S_{INC}(\varkappa, 0) = S^{D}_{INC}(\varkappa, 0) + S^{PH}_{INC}(\varkappa, 0) \tag{17a}$$

where

$$S^{D}_{INC}(\varkappa, 0) = \frac{1}{\pi D \varkappa^2} e^{-2W(\varkappa)} \tag{17b}$$

and

$$S^{PH}_{INC}(\varkappa, 0) = \frac{\hbar^2 \varkappa^2}{2M} e^{-2W(\varkappa)} \, 3 \frac{T}{\theta_D} \quad . \tag{17c}$$

In fig. 12 is shown $\varkappa^2 S_{INC}(\varkappa, 0)$ and the deduced $\varkappa^2 S^{D}_{INC}(\varkappa, 0)$ for liquid H_2. It is seen that an interpretation according to eq. 16 is not consistent with the observed $S_{INC}(\varkappa, \omega)$, since a horizontal line is not observed. Interpretation according to eq. 17b agrees well with the result deduced independently from the coherent data. Consequently it is not necessary to distinguish between the two Debye-Waller factors, defined independently through the ACB sum rule in eq. 8 and through eq. 11b.

Finally the one phonon density of states $Z(\omega)$ may be deduced from eq. 11c. As mentioned above $Z(\omega)$ should for small values of ω approach its Debye value $Z_D(\omega)$, but for all values of ω a stringent test on the validity of $Z(\omega)$ is provided if one calculates $Z(\omega)$ for different $\varkappa$'s. This is shown in fig. 13 for liquid H_2. The result shows that $Z(\omega) \simeq Z_D(\omega)$ for $\hbar\omega < 3$ meV

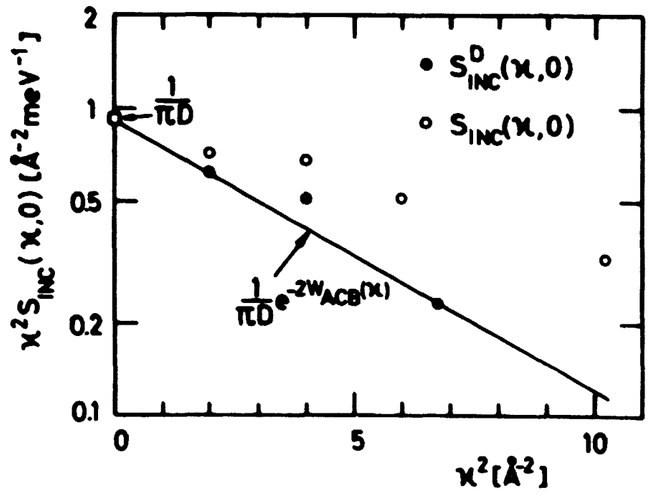

Fig. 12. $S(\varkappa, 0)$ for liquid H_2 analysed according to the two interpretations discussed in the text. ☐ indicates independent result using $D = 4.7 \times 10^{-5}$ cm^2/s, and the solid line indicates the result from coherent scattering.

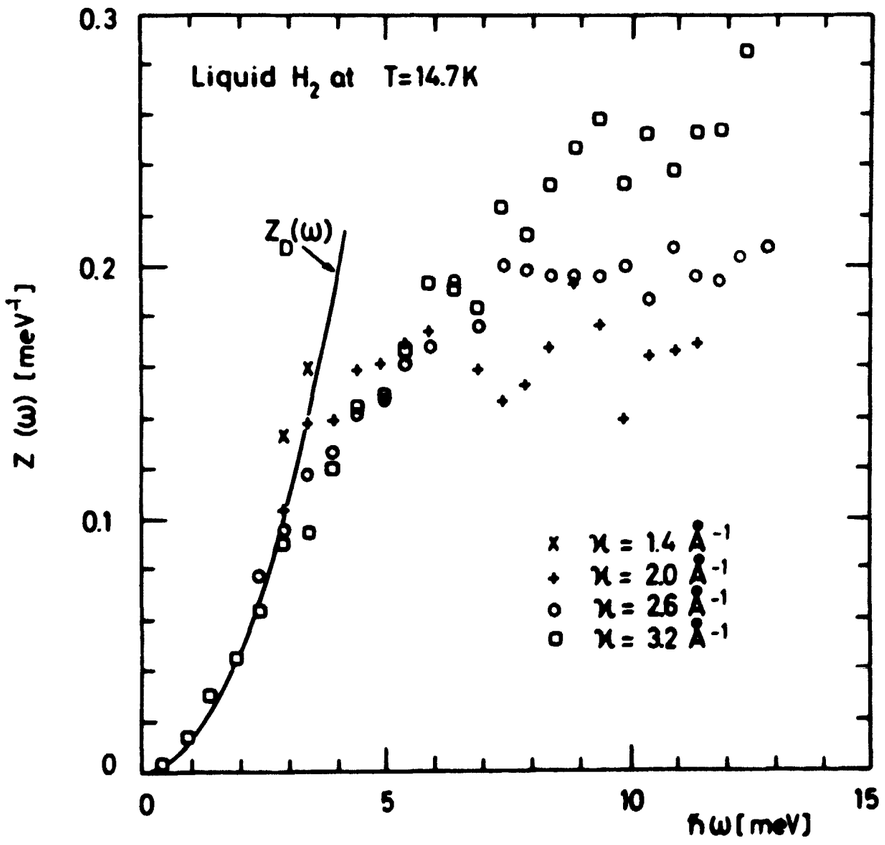

Fig. 13. Density of one-phonon states $Z(\omega)$ for liquid H_2 deduced from $S_{INC}(\varkappa, \omega)$.

and that $Z(\omega)$ is well defined up to $\hbar\omega \simeq 7$ meV. For larger energies fig. 13 indicates that multiphonon, which has not been included in the analysis, increases with increasing wavevectors. This is observed also in liquid ^{4}He and agrees with conventional multiphonon theories. Unfortunately the multiphonon region was not investigated in the present experiment.

3.3. Discussion of Liquid H_2

In the analysis of the neutron scattering from liquid H_2 at 14.7 K as represented by the normalized scattering laws $S_{COH}(\varkappa, \omega)$ and $S_{INC}(\varkappa, \omega)$, the result strongly suggests that phonon-like excitations exist in this liquid. These excitations are well characterized by the Debye temperature $\theta_D \sim 70$ K as observed through the coherent spectrum and the deduced one-phonon density of states $Z(\omega)$. θ_D is in agreement with a scaling to the solid through the Gruneisen relation. Further a Debye-Waller factor may be defined and independent calculations of the ACB sum rule, the contribution to the scattering from self diffusion, and $Z(\omega)$ yield consistently the mean square displacement $\langle u^2 \rangle = 0.62$ Å^2, compared with $\langle u^2 \rangle = 0.48$ Å^2 in the solid. In contrast to liquid A, a consistent analysis cannot be carried out without introducing the concept of phonons, as contributing to the neutron scattering from liquid H_2.

As discussed in sections 2.4 and 2.6, liquid H_2 may be classified as a low temperature Lennard-Jones liquid. Since MD calculations on these liquids can be performed, it is natural to predict the possible result of such a calculation. In fig. 14 is therefore shown the symmetrized coherent scattering law $\tilde{S}_{COH}(\varkappa, \omega)$ obtained from $S_{COH}(\varkappa, \omega)$ similarly to eq. 13. Together with $\tilde{S}_{INC}(\varkappa, \omega)$ shown in fig. 10, $\tilde{S}_{COH}(\varkappa, \omega)$ is the expected result of a classical calculation. The problem, however, arises of how to define the state T^*, ρ^* for liquid H_2, and a crude estimate is the following. Owing to quantum effects, the potential parameters σ_{LJ} and ε_{LJ} must be renormalized to σ'_{LJ} and ε'_{LJ}. From $S(\varkappa, 0)$ in fig. 8 it seems natural to estimate $\sigma'_{LJ} = 3.4$ for H_2, since then $\sigma_{LJ} \varkappa_0 = 6.8$ is obeyed for both liquid A and liquid H_2. ε'_{LJ} is then obtained from the value of D, using the MD result of Verlet et al.[31]. Extrapolating their calculations one gets consistently that ε_{LJ} may be renormalized to $\varepsilon'_{LJ} = 172$ K. With σ'_{LJ} and ε'_{LJ} the state of liquid H_2 at 14.7 K is defined by $\rho^* = 0.35$ and $T^* = 0.085$, differing significantly from the values given in table 2.

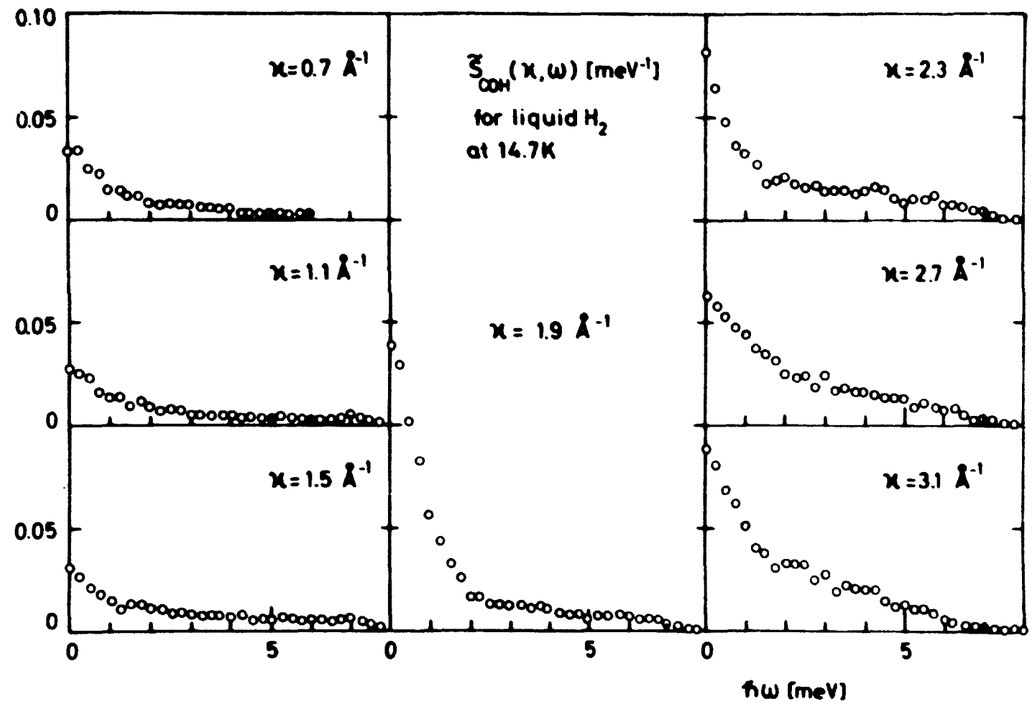

Fig. 14. Symmetrized coherent scattering law $\tilde{S}_{COH}(\varkappa, \omega)$ for liquid H_2.

4. NEUTRON SCATTERING IN LIQUID N_2 AT 66.4 K

Among the classes of liquids defined in chapter 2 that of classical Lennard-Jones liquids is the most strictly defined. The potential parameters ε_{LJ} and σ_{LJ} can be determined from measurements in the gas phase, and together with the mass M they should allow a first principles' theory to be established. Although the Lennard-Jones potential is generally recognized to be a good average potential, more sophisticated potentials have been worked out to account for finer details in experimental results. The purpose of this chapter is to present neutron scattering results from liquid N_2, and to test whether the dynamical behaviour of this liquid scales appropriately to that of liquid A, measured by Sköld et al.[8].

Only the dynamical behaviour of the molecular centres is of interest for this discussion. As will be shown below, it can be deduced from the neutron scattering pattern. It should, however, be mentioned that recently considerable interest has been devoted to the general dynamical behaviour of

the condensed phases of molecular nitrogen. MD results have been published for the liquid phase[32] and larger computations are in progress, NS results from liquid N_2 of which those reported here are only a part will be published[33], and further a NS study of solid N_2 has been undertaken by Kjems et al.[34].

4.1. Neutron Scattering Properties of Molecular Nitrogen

The neutron scattering properties of molecular nitrogen differ drastically from those of molecular hydrogen. The larger moment of inertia of the N_2 molecule, makes the energy of the first rotational state $\Delta E = 0.49$ meV = 5.7 K, compared with the liquid temperature of 66.4 K. ΔE together with the parameters introduced below have been defined in chapter 3. It is therefore natural to consider the N_2 molecule as a totally classical rotator, neglecting the differences between the ortho and para states of the molecule.

For small wavevectors however, the coherent neutron scattering cross sections from H_2 and N_2 are similar. Here the molecule may be considered as a point scatterer with a scattering length of $2b_{COH}j_0(\varkappa d/2)$, where $d = 1.094$ Å for N_2; but whereas in the case of H_2 the incoherent scattering could be reduced to zero, this is not strictly true for N_2.

Sears[35] has calculated the cross sections for a classical system of diatomic homonuclear molecules. The cross section per molecule is found to be:

$$\frac{d^2\sigma}{d\Omega d\omega} = 2\frac{k}{k_0} e^{\frac{\hbar\omega}{2k_BT}} \frac{\sigma_{COH}}{4\pi} \times \{ a_{COH}(\varkappa)\tilde{S}_{COH}(\varkappa,\omega) + a_{INC}(\varkappa)\tilde{S}_{INC}(\varkappa,\omega) + \sum_{\ell=1}^{\infty} \{ a_\ell(\varkappa) \int_{-\infty}^{\infty} S_{INC}(\omega-\omega')S_\ell(\omega')d\omega' \} , \quad (18)$$

where $\sigma_{COH} = 11.1$ b is the coherent nuclear scattering cross section[36]. Because of the fact that liquid N_2 is considered to be almost classical, eq. 18 is written, so that the symmetrized scattering laws, discussed in the previous chapter, are shown. Not yet defined in eq. 18 is the rotational scattering law $S_\ell(\omega)$, which is the Fourier transform of the ℓ'th rotational relaxation function $F_\ell(t)$:

$$S_\ell(\omega) = \frac{1}{\pi} \int_0^\infty F_\ell(t)\cos(\omega t)dt . \quad (19)$$

Further the formfactors for each of the scattering laws in eq. 18 are the following:

$$a_{COH}(\varkappa) = 2j_0^2(\tfrac{\varkappa d}{2})$$

$$a_{INC}(\varkappa) = \frac{\sigma_{INC}}{\sigma_{COH}} j_0^2(\tfrac{\varkappa d}{2}) \quad (20)$$

$$a_\ell(\varkappa) = \begin{cases} (2\ell+1)\, j_\ell^2(\tfrac{\varkappa d}{2}) \{2 + \frac{\sigma_{INC}}{\sigma_{COH}}\}, & \ell \text{ even} \\ (2\ell+1)\, j_\ell^2(\tfrac{\varkappa d}{2}) \frac{\sigma_{INC}}{\sigma_{COH}}, & \ell \text{ odd} \end{cases}$$

In (20) j_ℓ is the ℓ'th spherical Bessel function and σ_{INC} is the nuclear incoherent cross section.

The main difficulty in calculating a_{INC} and the a_ℓ's lies in the uncertainty of σ_{INC} of which no accurate value has been published. From Willis[36] one can estimate $\sigma_{INC}/\sigma_{COH} \sim 0.03$, but from the results shown in section 4.2.2 it is natural to assume either $\sigma_{INC}/\sigma_{COH} = 0$ or $\sigma_{INC}/\sigma_{COH} = 0.048$. Consequently in interpreting the spectra, these two possibilities must be considered separately.

In fig. 15 are shown the relevant formfactors according to eqs. 18 and 20, presented for $\varkappa$-values of interest for the present study. Also shown is the sum of all a's neglecting incoherent scattering. Fig. 15 shows that for $\varkappa < 7$ Å^{-1} only the centre of mass motion through $\tilde{S}_{COH}(\varkappa,\omega)$ and the rotational transition of $\ell = 2$ (the "d-wave") play a significant role in the coherent scattering. For small wavevectors however, the incoherent scattering $a_{INC}\tilde{S}_{INC}(\varkappa,\omega)$ may contribute significantly. The total coherent scattering using the sum rule (5) is $a_{COH}S(\varkappa)$, compared with a_{INC} which according to eq. 9 measures the total incoherent scattering. Since $S(\varkappa) \sim 0.1$ for the $\varkappa < 1$ Å^{-1} the two contributions are comparable, if one uses the finite value of $\sigma_{INC}/\sigma_{COH}$ given above.

In analysing the data obtained for liquid N_2 one may proceed in the following way. From the scattering are deduced the nuclear scattering laws $\tilde{S}_{n,COH}(\varkappa,\omega)$ and $\tilde{S}_{n,INC}(\varkappa,\omega)$ defined similarly to the simple monoatomic case through the scattering cross section per nucleus:

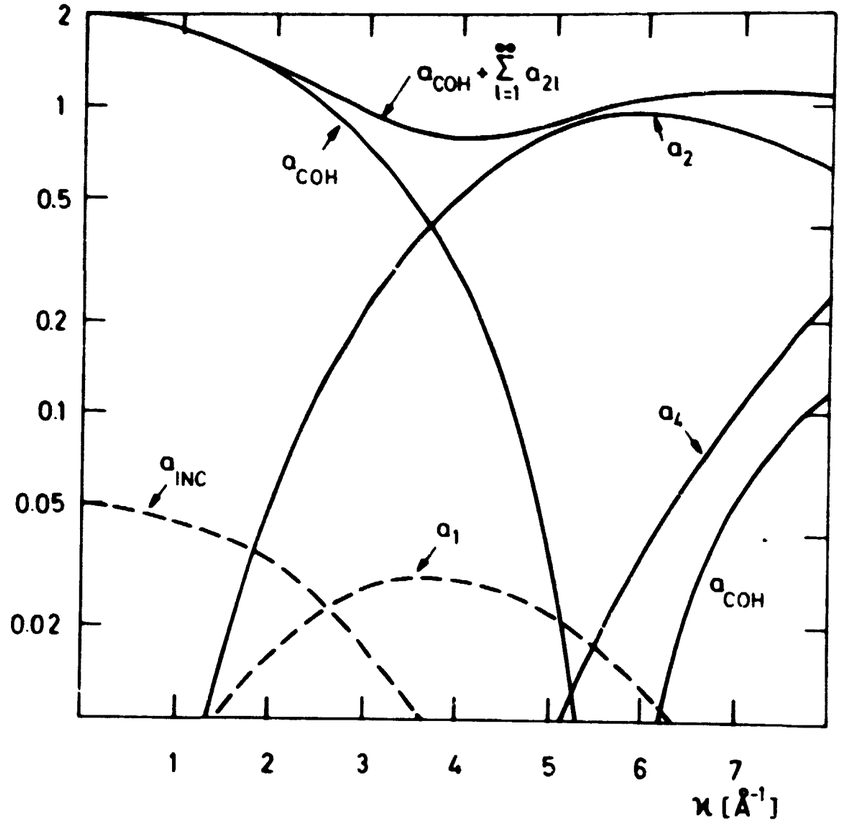

Fig. 15. Formfactors of interest for the interpretation of the cross section for molecular N_2. The dashed lines correspond to an estimate of $\sigma_{INC}/\sigma_{COH} = 0.048$ as discussed in the text.

$$\frac{d^2\sigma}{d\Omega\, d\omega} = \frac{k}{k_0}\, e^{\hbar\omega/(2k_BT)}\, \frac{\sigma_{COH}}{4\pi} \left\{ \tilde{S}_{n,\,COH}(\underline{\varkappa},\omega) + \frac{\sigma_{INC}}{\sigma_{COH}}\, \tilde{S}_{n,\,INC}(\underline{\varkappa},\omega) \right\} \tag{21}$$

According to eq. (18) and the discussion given above, the molecular scattering laws are then deduced from:

$$\tilde{S}_{n,\,COH}(\varkappa,\omega) = a_{COH}(\varkappa)\, \tilde{S}_{COH}(\varkappa,\omega) + a_2(\varkappa) \int_{-\infty}^{\infty} \tilde{S}_{INC}(\varkappa,\omega-\omega')\, S_2(\omega')\, d\omega' \tag{22a}$$

and

$$\tilde{S}_{n,\,INC}(\varkappa,\omega) = \frac{1}{2}\, a_{COH}(\varkappa)\, \tilde{S}_{INC}(\varkappa,\omega) \tag{22b}$$

From eq. 22 and the values of the formfactors shown in fig. 15 it appears that for 0 Å^{-1} < $\varkappa$ < 2.2 Å^{-1} $\tilde{S}_{COH}(\varkappa,\omega)$ is studied solely, whereas in the region 4.5 Å^{-1} < $\varkappa$ < 6.5 Å^{-1} information about $\tilde{S}_{INC}(\varkappa,\omega)$ and $S_2(\omega)$ is obtained. In the following the results will be presented and compared with the results of liquid A.

4.2. Experimental Results for Liquid N_2 at 66.4 K

4.2.1. The Structure Factor

In the case of liquid H_2 a brief discussion of the liquid structure factor for liquid N_2 will be given. As suggested by Sears[35], one may define both a nuclear structure factor $S_n(\varkappa)$, related to $\tilde{S}_{n,\,COH}(\varkappa,\omega)$ through eq. 5 and directly measured by a diffraction experiment, as well as a molecular structure factor $S(\varkappa)$ related similarly to $\tilde{S}_{COH}(\varkappa,\omega)$. Using eqs. 18 and 21 together with the sum rules (5) and (9) we get[35]:

$$S(\varkappa) - 1 = (S_n(\varkappa) - 1 - j_0(\varkappa d))/(2\, j_0^2(\tfrac{\varkappa d}{2})). \tag{23}$$

Fig. 16a presents the result of an analysis according to eq. 23. The data for liquid N_2 are taken from the X-ray measurements of Furumoto and Shaw[37], and they are compared to the neutron diffraction result of Yarnell et al.[38] for A, using scaling according to σ_{LJ}. When $2j_0^2(\frac{\varkappa d}{2}) = a_{COH}$ is small, reliable data for $S(\varkappa)$ cannot be obtained. Although the dominant feature of fig. 16a is agreement the fact that the second maxima for A and N_2 do not coincide, indicates an insufficiency in the scaling. Sears suggested that a difference in the $S(\varkappa)$'s might be due to a weak anisotropic coupling, a point discussed in the following sections.

An alternative use of eq. 23 is to take $S(\varkappa)$ from liquid A and to deduce $S_n(\varkappa)$. Using scaling, this function would in the absence of anisotropic interactions reproduce the measured $S_n(\varkappa)$ for N_2. From fig. 16b it is seen that the second maximum is shifted similarly to fig. 16a; but the fact that the two S_n's do not coincide in the region $18 \leq \varkappa \cdot \sigma_{LJ} \leq 26$ cannot be explained by Sears's formulation. In this region, corresponding to 4.8 Å$^{-1} \leq \varkappa \leq 7$ Å^{-1} for liquid N_2, any contribution to $S_n(\varkappa)$ from $S(\varkappa)$ is effectively suppressed, so that equation 23 reduced to $S_n = 1 + j_0(\varkappa d)$. However, a smooth maximum at $\varkappa \cdot \sigma_{LJ} \sim 22$ occurs, in addition to the maximum at $\varkappa \cdot \sigma_{LJ} = 28$ as prescribed by eq. 23. The existence of this unexpected maximum has recently been verified by neutron diffraction[39].

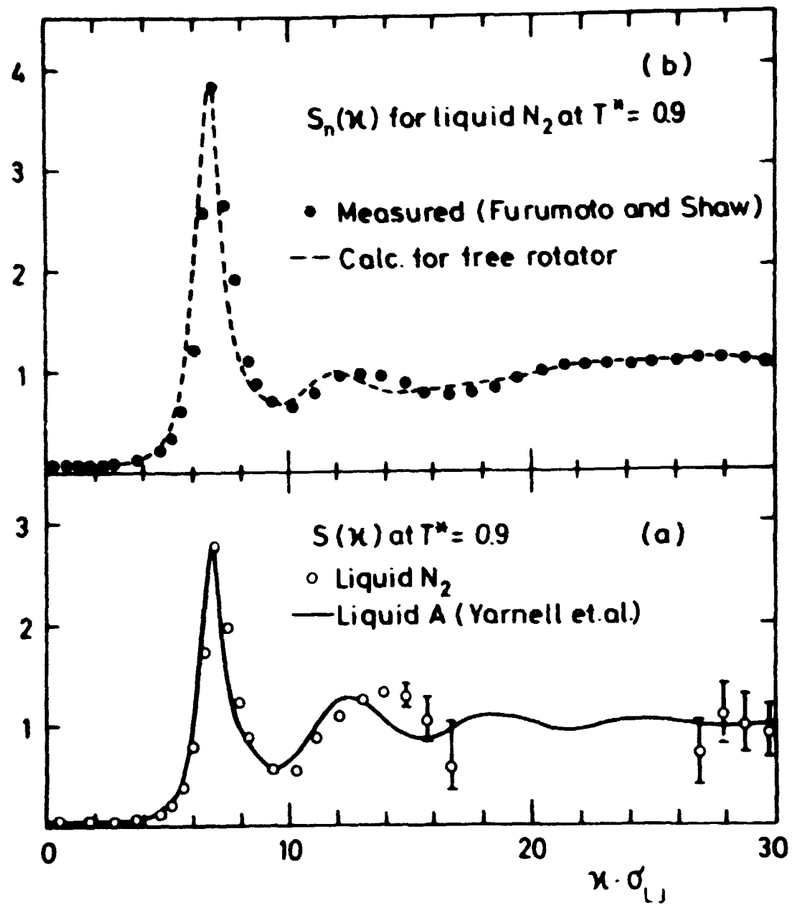

Fig. 16. Comparison between the liquid structure factors measured in liquid A and liquid N_2.

4.2.2. Collective Motion

The results of the neutron scattering experiment for liquid N_2 are shown in fig. 17 in the shape of the nuclear scattering law $\tilde{S}_{n,COH}(\varkappa, \omega)$ for the wavevectors $\varkappa$ = 0.1, 1.0, 1.3, 1.6, 1.9, 2.2, 4.0, 4.8, 5.6, and 6.4 Å^{-1}. Except for the smaller $\varkappa$-value the spectra were corrected in the way described in the Appendix. $\tilde{S}_{n,COH}(\varkappa, \omega)$ was normalized using eq. 5 and the measured $S_n(\varkappa)$ shown in fig. 16. For $\varkappa$ = 1.0 Å^{-1} and $\varkappa$ = 1.3 Å^{-1}, the measured spectra are in a natural way divided into a narrow line and a broader one. Since the width of the narrow line fulfuls eq. 12 for simple diffusion, where D is determined independently as shown in section 4.2.3, this portion of the spectra may be due to incoherent scattering if

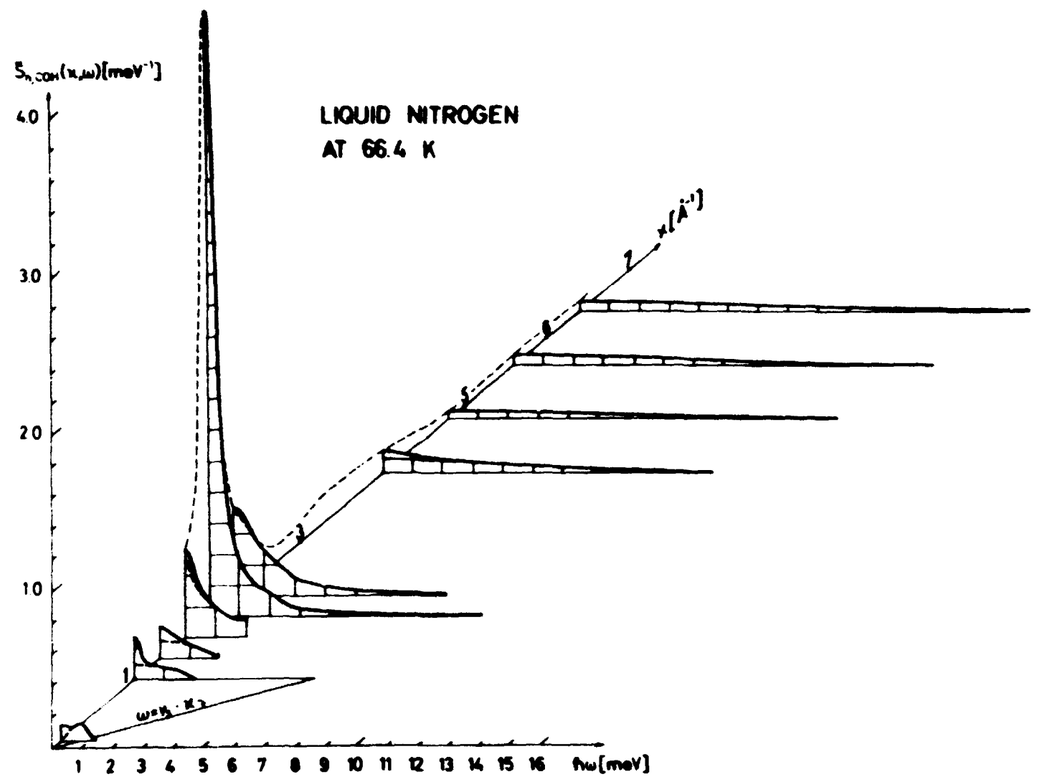

Fig. 17. Coherent scattering law for liquid N_2 at 66.4 K. The dashed lines show the corrected scattering law if a possible incoherent scattering is subtracted as discussed in the text. At $\varkappa$ = 4.0 Å^{-1} the scattering is separated according to the formfactors shown in fig. 16.

$\sigma_{INC}/\sigma_{COH}$ = 0.048. This value gives according to eq. 21 the a correct division of the spectra. Subtracting the possible incoherent scattering, one obtains for small wavevectors an alternative $\tilde{S}_{n,COH}(\varkappa, \omega)$, as mentioned in section 4.1.

Only for $\varkappa$ = 0.1 Å^{-1}, is a small peak in $\tilde{S}_{n,COH}(\varkappa, \omega)$ for $\omega \neq 0$ seen. This region, only investigated through the experimentally difficult small angle scattering, corresponds to wavevectors where the sound wave according to linear hydrodynamic theory for viscous fluids should be overdamped[9]. Since most of the width of the line centred around $\omega = v_s \cdot \varkappa$, where v_s is the sound velocity, is due to experimental resolution, the result indicates that fairly well-defined sound waves exist in liquid N_2 at $\varkappa$ = 0.1 Å^{-1}. At $\varkappa$ = 0.23 Å^{-1} Levesque et al.[9] in a MD calculation found a broad inelastic line qualitatively in agreement with the present NS result.

The MD result could be well understood by introducing a coupling between longitudinal and transverse waves, often neglected in fluid mechanics. Since the same theory can explain the tails found in the velocity autocorrelation function in dense fluids[40], an NS result is of interest as a direct experimental verification of the MD results and the mentioned theory. The quality of the present result does however not permit this verification to be conclusively made.

For wavevectors $\varkappa \geq 1$ Å^{-1} no evidence is found for well defined collective excitations in liquid N_2, since no inelastic peak is seen in $\tilde{S}_{n,COH}(\varkappa, \omega)$, for constant values of $\varkappa$. This conclusion is independent of the possible contribution from incoherent scattering, and in this respect N_2 is in qualitative agreement with A. Quantitatively the results for the two liquids may be compared when $\tilde{S}_{COH}(\varkappa, \omega)$ is deduced from eq. 22 and scaled according to σ_{LJ} and τ_{LJ}. This may be unambiguously done e.g. for $\varkappa = \varkappa_0$, corresponding to 1.9 Å^{-1} and 2.0 Å^{-1} for N_2 and A respectively. Fig. 18 shows the results of the comparison. It should be noted that no adjustable parameters were used.

The detailed agreement between the result for the two liquids at $\varkappa = \varkappa_0$ for $0.3 \lesssim \omega \cdot \tau_{LJ} \lesssim 2.2$, corresponding to 1 meV $< \hbar\omega <$ 6.7 meV in liquid N_2, is a strong indication that the isotropic Lennard-Jones potential is appropriate for the two liquids concerning their dynamical behaviour. For larger energies the N_2 data are probably inaccurate owing to multiple scattering effects, discussed in the Appendix.

The significant deviation between the two $\tilde{S}_{COH}(\varkappa, \omega)$'s for small values of ω may be explained in terms of an anisotropic interaction due to rototranslational coupling in liquid N_2. Although this cannot be conclusively stated it seems plausible, when one compares the frequencies at which the $\tilde{S}_{COH}(\varkappa, \omega)$'s for A and N_2 disagree with the characteristic classical rotational frequency of the N_2 molecule. The latter corresponds to an energy of $\hbar(k_B T/I)^{1/2} = 0.22$ meV where I is the molecular moment of inertia[35]. Compared with the energy where agreement occurs at $\hbar\omega = 1$ meV, this indicates that disagreement between A and N_2 occurs at time scales comparable to or larger than the classical rotation period of the N_2 molecule. This result also found at other $\varkappa$-values supports the suggestion that the deviation from scaling is due to anisotropic interactions, whereas the isotropic part of the interaction potential is well described by σ_{LJ} and ε_{LJ}.

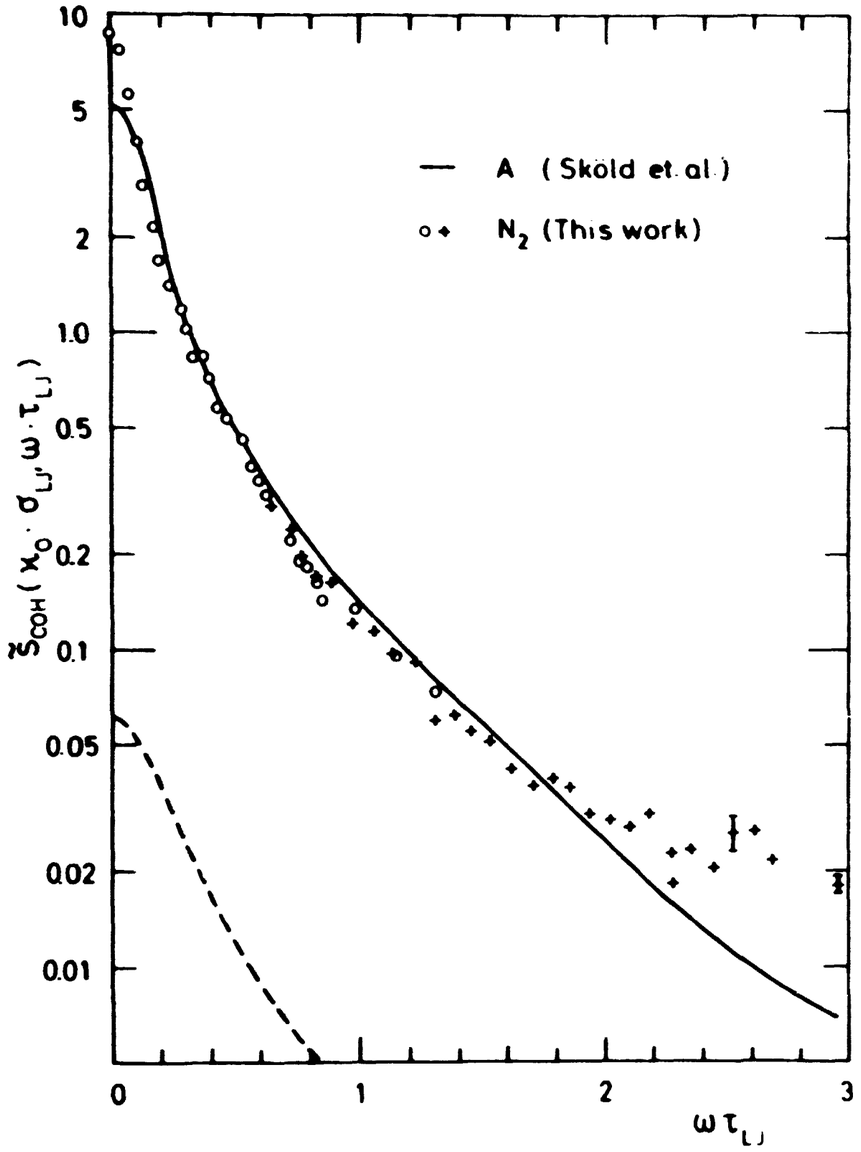

Fig. 18. Comparison between $\tilde{S}_{COH}(\varkappa_0, \omega)$ for the two liquids A and N_2. The levelling-off of the N_2 data is estimated to be due to multiple scattering. The dashed line shows possible contribution from incoherent scattering.

Since the deviation from scaling occurs at small frequencies, $S_{COH}(\varkappa, 0)$ is not expected to agree for liquid A and liquid N_2. In fig. 19 this function is compared for the two liquids. In contradistinction to the structure factor $S(\varkappa)$, a large deviation is seen even around the first peak at $\varkappa = \varkappa_0$ when the function $S_{COH}(\varkappa, 0)$ is studied. Similarly significant deviations

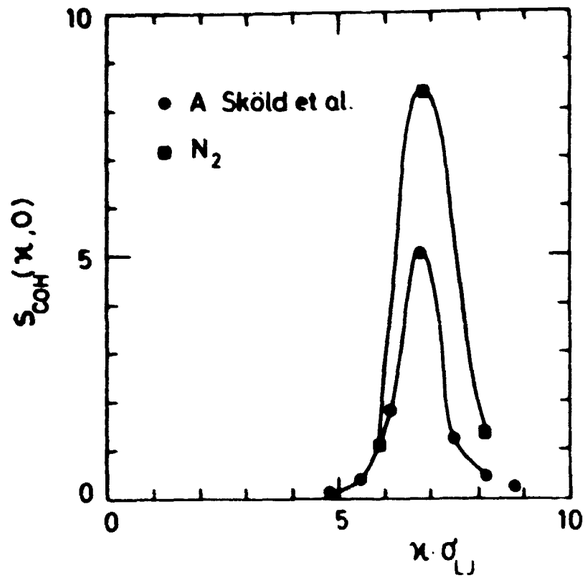

Fig. 19. Comparison of $S_{COH}(\varkappa, 0)$ for the two liquids A and N_2.

are seen in the scaled FWHM of $S_{COH}(\varkappa,\omega)$. This evidence indicates that the agreement obtained for $S(\varkappa)$ may be fortuitous. MD results[31] showing local anisotropy in the pair distribution function seem to indicate this also.

4.2.3. Single-Particle Motion

As discussed above, the scattering at wavevectors $4.0\ \text{Å}^{-1} \leq \varkappa \leq 7.0\ \text{Å}^{-1}$ consists mainly of a contribution from the last term in eq. 22a. In this region one has to consider both $\tilde{S}_{INC}$ and S_ℓ, which considerably limits the information that can be gained about the two functions.

In order to analyse the data, models were used for the two scattering laws. $S_{INC}(\varkappa,\omega)$ was assumed to be described by simple diffusion according to eq. 10. Similarly it can be shown to be a reasonable assumption[33] that $S_\ell(\omega)$ is well described by rotational diffusion, according to which[35]:

$$S_\ell(\omega) = \frac{1}{\pi} \frac{(\ell+1) D_r}{(\ell(\ell+1)D_r)^2 + \omega^2} \qquad (24)$$

where D_r is the rotational diffusion coefficient. Inserting eqs. 24 and 10 into the last term in eq. 22a we get the result for the full width at half maximum:

$$\text{FWHM} = 12\, D_r + 2D\varkappa^2 , \qquad (25)$$

From eq. 25 D_r and D may be determined. This is done in fig. 20, yielding $D_r = 0.82\ (\text{ps})^{-1}$ and $D = 2.7 \cdot 10^{-5}\ \text{cm}^2/\text{s}$. Only the value of the self diffusion coefficient D is of importance for the discussion here, and it compares well with the scaled MD result[31] of $3.0 \cdot 10^{-5}\ \text{cm}^2/\text{s}$ and reasonably with the estimate of Sears[35] giving $D = 3.7 \cdot 10^{-5}\ \text{cm}^2/\text{s}$ at the boiling point. In liquid A[8] $D = 1.94 \cdot 10^{-5}\ \text{cm}^2/\text{s}$ scales well to both MD and the value for N_2.

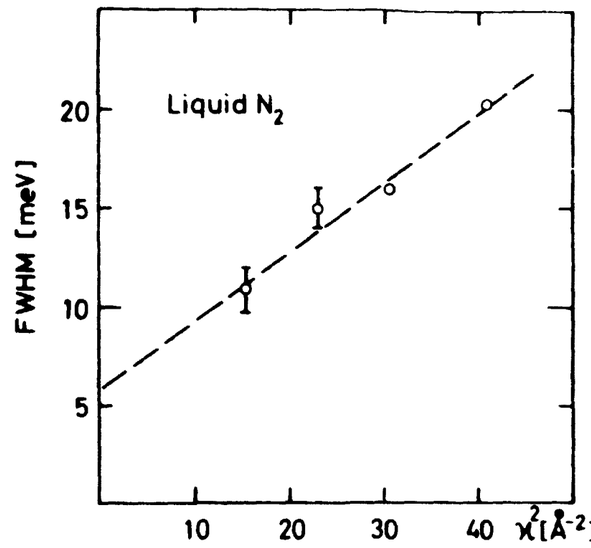

Fig. 20. FWHM of $\tilde{S}(\varkappa,\omega)$ for $4\text{Å}^{-1} \leq \varkappa \leq 6.4\ \text{Å}^{-1}$, obtained as a fit to Lorentzian lines shapes.

Consequently the limited information gained about the single particle excitations of the molecular centres in liquid N_2 leads to the conclusion that scaling is obeyed according to σ_{LJ} and ε_{LJ}.

4.3. Discussion of Liquid N_2

The result of neutron scattering in liquid N_2 has been analysed through the normalized molecular scattering laws $\tilde{S}_{COH}(\varkappa,\omega)$ and $\tilde{S}_{INC}(\varkappa,\omega)$, assuming a simple model for the rotational relaxations in this liquid. Both the collective excitations and the single-particle excitations scale well with

NS results from liquid A[8] and with MD results[9, 31], according to the molecular Lennard-Jones parameters. This supports the classification made in chapter 2, according to which the Lennard-Jones liquids are not expected to support well-defined, short-wavelength excitations. However, the preliminary result at $\varkappa = 0.1$ Å^{-1} indicates that the sound wave persists up to this wavevector in liquid N_2. Considerable interest and discussions have been devoted to the analysis and understanding of related phenomena in dense fluids[9].

The significant deviation from scaling in liquid N_2 at small energies is to some extent unexpected. Since the molecular ordering temperature is T = 35.6 K in the solid phase, one might not expect the short range anisotropic interactions to be of importance at liquid temperatures. Further the small bond length d = 1.094 Å compared with σ_{LJ} = 3.7 Å makes the geometrical shape of the N_2 molecule rather isotropic. The experimental evidence provided through NS[33] and MD[32] results shows, however, that the anisotropic part of the interaction potential cannot be neglected.

5. CONCLUSION

In the two previous chapters NS results from the liquids H_2 and N_2 relevant for the dynamical behaviour of the molecular centres have been presented and discussed. In liquid H_2, the concept of phonons must be introduced together with the concept of self diffusion in order to interpret the data consistently. The Debye-Waller factor, the Debye temperature and the density of one-phonon states can be deduced and agree well with the results from the solid[12] scaled to the density of the liquid. Further the measured self diffusion coefficient agrees with the previously published value[22].

Less extensive results from liquid N_2 indicate that besides an anisotropic contribution to the interactions the dynamical behaviour of the molecular centres is well described by the isotropic Lennard-Jones potential parameters, so that the results from A and N_2 scale appropriately. In these liquids one cannot from the NS data rigorously deduce any of the characteristics of phonons. It should at this point be emphasized that the discussion here has been kept to the normalized density-density correlation functions as measured by an NS experiment, whereas introduction of e.g. the velocity-velocity correlation functions may easily lead to false conclusions. Further in confining the analysis to correlation functions, one avoids the problems of the detailed movements of the atoms in the liquid, without loosing any

physical insight, possibly gained through the experiments.

In liquid Rb, NS[6] and MD[7] results show that phonon-like excitations exist in this liquid, although less pronounced than in liquid H_2. A preliminary analysis in terms of sum rules indicates that a one-phonon part of the spectra cannot be isolated in liquid Rb, but a solid-like dispersion curve for the excitations may be deduced.

The experimental evidence supports the classification presented in chapter 2. The classes seem uniform and well separated from each other when their dynamical behaviour is analysed. In quantum liquids, classified according to table 1 and fig. 1 as low temperature, anharmonic liquids the phonons are quantitatively well defined. Less pronounced is the phonon-like behaviour in the high temperature, harmonic liquid, available for experimental study in the case of metallic liquids. Finally in the case of the high temperature, anharmonic liquids, the results for the Lennard-Jones liquids show that the phonons cannot survive when all four assumptions basic for the exact phonon theory are violated.

Consequently the following has been learnt about the collective exitations in liquids. The existence of phonon-like collective excitations depends critically on the temperature as measured by T/θ_D, where θ_D is the Debye temperature, together with the details of the form of the interaction potential. In contradistinction to what has often been anticipated the fact that the diffusion process occurs at time scales similar to those of the possible phonons does not seem to have any drastic effect on the collective excitations in the liquid phase. Finally it is worth noting that the effect of non-periodicity is a significant change in the phonon spectra[13, 16], which may explain the reported specific heat anomaly at very low temperatures in amorphous systems[14].

According to table 1 and the discussion in chapter 2 the breakdown of three out of four assumptions has been studied and can be conceptually understood. Non-stationarity as well as high temperatures and anharmonic interactions tend to destroy the phonons, but only when all three effects are present does the concept of phonons lose its meaning. Concerning diffusion, however, it cannot be considered satisfactory that the effect on the collective excitations, has not been seen. Since the phonon spectra characterized by θ_D are not expected to vary much with temperature, whereas the diffusion coefficient D varies exponentially with T according to Arrhenius' law, this effect should be a simple temperature effect for any particular liquid. However, as discussed in chapter 2, the most fruitful results are expected from supercooled liquids.

Neglecting the classification according to table 1, the dynamical behaviour in simple liquids close to their triple points appears to be conceptually difficult to understand. Such a classification may therefore be useful in the absence of good theories derived from first principles. On the other hand it is encouraging that such theories have appeared as extensions of the ordinary hydrodynamic theory[9], but in order to test these theories, NS experiments must be performed for smaller wavevectors. The preliminary result for liquid N_2, shown in section 4.2.2, points towards small angle scattering as a new and challenging field in NS.

Finally it should be emphasized that the materials discussed in this report constitute only a very small fraction of the interesting and available non-crystalline materials. The conclusion of the report is however that even the most simple liquids must on experimental evidence be classified according to table 1 if a microscopic understanding of their different dynamical behaviour should be understood. On the other hand, conceptual understanding along the lines discussed here justifies the study of more complicated (or realistic) liquids especially if both MD and NS experiments can be made. It seems therefore promising to study the condensed phases of nitrogen through combined efforts from many laboratories[32, 34]. In the near future perhaps, water[41] could be the subject of a similar collaboration, based on the knowledge gained from the materials studied in this report. Much of the interpretation of experimental results obtained from complicated (or "real") materials seems to suffer from lack of precise knowledge of the simple systems.

ACKNOWLEDGEMENTS

Professor A. R. Mackintosh suggested the general line of research described in this thesis, and encouraged the author in carrying it out.

The work was carried out at the Physics Department of the Danish Atomic Energy Research Establishment Risø, and the author wishes to express his gratefulness to the members of the neutron scattering group for assistance and advice throughout the study. Further the technical staff of the low temperature group is thanked for their never failing assistance with the low temperature apparatus.

The inspiring collaboration with professor J. P. McTague of the Chemistry Department, University of California Los Angeles, is gratefully acknowledged.

The author wishes to thank professor A. Sjölander, Chalmers Tekniska Högskola, and dr. A. Rahman, Argonne National Laboratory, for their interest in the work and for helpful suggestions.

REFERENCES

1) D.G. Henshaw and A.D.B. Woods, Phys. Rev. 121 (1961) 1266-1274.

2) P.A. Egelstaff, Rep. Progr. Phys. 29 (1966) 333-345.

3) K. Skold and K.E. Larsson, Phys. Rev. 161 (1967) 102-116.

4) R.A. Cowley and A.D.B. Woods, Can. J. Phys. 49 (1971) 177-200.

5) K. Carneiro, M. Nielsen, and J.P. McTague, Phys. Rev. Lett. 30 (1973) 481-485.

6) J.R.D. Copley and J.M. Rowe, Phys. Rev. Lett. 32 (1974) 49-52.

7) A. Rahman, Phys. Rev. Lett. 32 (1974) 52-54.

8) K. Sköld, J.M. Rowe, G. Ostrowski, and P. Randolph, Phys. Rev. A 6 (1972) 1107-1131.

9) D. Levesque, L. Verlet, and J. Kürkijarvi, Phys. Rev. A 7 (1973) 1690-1700.

10) J.M. Rowe and K. Sköld, In: Neutron Inelastic Scattering, Grenoble, 6-10th March 1972, (IAEA, Vienna, 1972) 413-433.

11) V.J. Minkiewicz, T.A. Kitchens, G. Shirane, and E.B. Osgood, Phys. Rev. A 8 (1973) 1513-1528.

12) M. Nielsen, Phys. Rev. B 7 (1973) 1626-1635.

13) K. Kim and M. Nelkin, Phys. Rev. B 7 (1973) 2762-2771.

14) R.B. Stephens, Phys. Rev. B 8 (1973) 2896-2905.

15) R.O. Pohl, private discussion.

16) J.D. Axe, D.T. Keating, G.S. Cargill III, and R. Alben, in press.

17) D.G. Carlson, J. Feder, and A. Segmüller, Phys. Rev. A 9 (1974) 400-403.

18) J.H. Jensen, Phys. kond. Mater. 13 (1971) 273-296.

19) S.A. Rice, J.P. Boon, and H.T. Davis, In: Simple Dense Fluids, Edited by H.L. Frisch and Z.W. Salsburg (Academic Press, New York, 1968) 290.

20) K. Carneiro and M. Nielsen, to be published.

21) G. Sarma In: Inelastic Scattering of Neutrons in Solids and Liquids, Vienna 11-14th October 1960 (IAEA, Vienna, 1961) 397-409.

22) P.A. Egelstaff, B.C. Haywood, and F.J. Webb, Proc. Phys. Soc. 90 (1967) 681-696.

23) L. de Graf and B. Moser, in press.

24) F.J. de Wette and A. Rahman, Phys. Rev. 176 (1968) 786.

25) V. Ambegaokar, J.M. Conway, and G. Baym, In: Lattice Dynamics, Copenhagen, 5-9th August 1963. Edited by R.F. Wallis (Pergamon, New York, 1968) 261-270.

26) K. Carneiro and M. Nielsen, In: Anharmonic Lattices, Structural Transitions, and Melting, edited by T. Riste (Nordhoff, Leiden, 1974) 349-362.

27) K. Carneiro, M. Nielsen, and J.P. McTague, In: Proceedings of the 24th Annual Meeting of "Societe de Chimie Physique", in press.

28) A Sjölander, In: Thermal Neutron Scattering. Edited by P.A. Egelstaff (Academic Press, New York, 1965) 291-345.

29) P. Schofield, Phys. Rev. Lett. 4 (1960) 239-240.

30) W. Marshall and S.W. Lovesey, Theory of Thermal Neutron Scattering (Oxford University Press, Oxford, 1971) 599 pp.

31) D. Levesque and L. Verlet, Phys. Rev. A 2 (1970) 2514-2528.

32) J. Barojas, D. Levesque, and B. Quentrec, Phys. Rev. A 7 (1973) 1092-1105.

33) K. Carneiro and J.P. McTague, to be published.

34) J. Kjems, private communication.

35) V.F. Sears, Can. J. Phys. 44 (1966) 1279-1297 and 1299-1311.

36) Chemical Applications of Thermal Neutron Scattering (Oxford, 1973) 296.

37) H.W. Furumoto and C.H. Shaw, Phys. Fluids 7 (1964) 1026-1029. Tabulated by P.W. Schmidt and C.W. Tompson, In: Simple Dense Fluids. Edited by H.L. Frisch and Z.W. Salsburg (Academic Press, New York, 1968). The author feels that the value of κ given in this reference should be multiplied by 2 in order to obtain a reasonable result.

38) J.L. Yarnell, M.J. Katz, R.G. Wenzel and S.H. Koenig, Phys. Rev. A 7 (1973) 2130-2144.

39) J. Dore and D.I. Page, to be published.

40) A. Rahman, Phys. Rev. A 136 (1964) 405-411.

41) A. Rahman and F.H. Stillinger, J. Chem. Phys. 55 (1971) 3336-3359.

42) H. Bjerrum Møller and M. Nielsen, In: Instrumentation for Neutron Inelastic Scattering Research. Proceedings of a Panel, Vienna, 1-5th December 1969 (IAEA, Vienna, 1970) 49-76.

43) T. Riste, same as ref. 42, 91-104.

44) I.A. Blech and B.L. Averbach, Phys. Rev. A 137 (1965) 1113-1116.

45) J.R.D. Copley, D.L. Price, and J.M. Rowe, Nucl. Instrum. Meth. 107 (1973) 501-507.

APPENDIX

THE STUDY OF LIQUIDS BY MEANS OF A TRIPLE AXIS SPECTROMETER

In an inelastic neutron scattering experiment the aim is to obtain quantitatively the two scattering laws $S_{COH}(\varkappa, \omega)$ and $S_{INC}(\varkappa, \omega)$ in a certain wavevector and energy region. Unlike in solids, where most often the positions of sharp excitations are studied, the functional form of the two scattering laws is of importance in liquids. This requires a good understanding of how to correct raw data for instrumental effect as well as other disturbing influences.

Most of the neutron scattering work on liquids has been performed on neutron time of flight spectrometers (TOF) as the total line shapes of the scattering laws are easily collected on this instrument. However, the procedure for conversion of the TOF-spectra in to constant $\varkappa$-scans is not efficient, whereas such scans can easily be performed on a triple axis crystal spectrometer (TAS). Since the relevant physical parameters are most easily extracted when the scattering laws are presented for constant $\varkappa$'s, this feature is in favour of choosing a TAS. The experiments reported here are performed on this latter instrument, and below is given a brief discussion of the instrumental precautions and corrections necessary in the study of liquids.

In fig. A1 a TAS is shown together with the parameters describing the instrument. Each of the four Soller slit collimators is defined by a horizontal and a vertical angular width σ_i and σ_{iv}, and the monochromator and analyser crystals are specified through lattice vector τ, mosaic spread η, thickness t, the structure factor for the Bragg reflection F, and finally the unit cell volume V. The Bragg reflection angles are denoted θ. Further in fig. A1 is shown the scattering diagram defining the scattering process as presented in section 3.1.

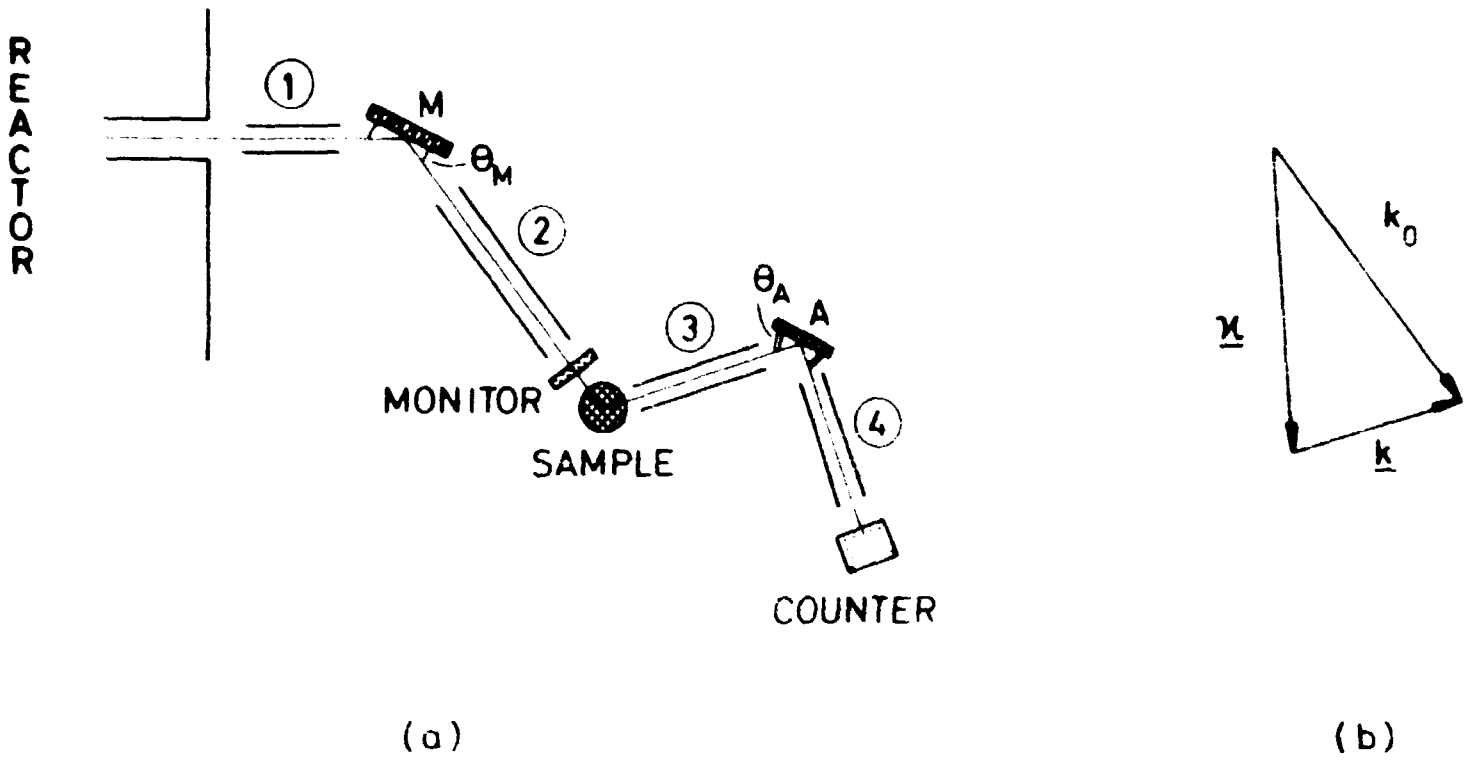

Fig. A1. Schematic diagram for the triple axis spectrometer. M = Monocromator Crystal, A = Analyser Crystal, and circles show the position of the collimators.

A.1. Higher-Order Crystal Reflections

One basic problem of the TAS is the appearance of higher-order reflections in the monocromator and analyser systems. Since the whole spectrum is to be measured one cannot be satisfied with the solution often used in crystal investigations, viz. that of choosing circumstances so that intensity due to higher order reflections falls in regions which are not of interest in the experiment. In the study of liquids it is therefore necessary to use very pure incoming beams obtained by means of neutron filters or monocromator crystals with forbidden reflections.

A.2. Treatment of the Resolution Function

When scans are performed the intensity counted $I(\varkappa,\omega)$ in the analysing system is related to the scattering laws through a convolution of the double differential cross section $d^2\sigma/(d\omega d\Omega)$ and the resolution function R of the TAS. R is conveniently divided into a sensitivity part, R_1, and a resolution part R_2. R_1 then describes the intensity corrections to the measured spectra related to the volume of R, and R_2 kept at volume unity describes the instrumental resolution width. In liquids only the energy width is of practical importance. The absolute magnitudes of R_1 and R_2 can be measured using the elastic incoherent scattering from a vanadium sample for which[8]:

$$\frac{d\sigma}{d\Omega} = \frac{\sigma_{INC}}{4\pi} e^{(-a\varkappa^2)} \qquad (A1)$$

where σ_{INC} = 5.13 barns and a = 0.00677 $Å^2$ at room temperature. Of major interest is therefore the relative variation of R_1 for the two modes in which the TAS is most conveniently operated, together with the influence of the finite energy resolutions described by R_2.

A.2.1. The Sensitivity Function R_1

In specific constant $\varkappa$-scans on a TAS, two special cases are of interest. They are the analyser scans (the EA mode) and the monocromator scans (the EM mode). In the EA mode of the instrument the incoming energy is kept fixed, and consequently higher-order neutrons are easily filtered out. If the cross section is assumed to be of the form:

$$\frac{d^2\sigma}{d\omega d\Omega} = \frac{\sigma}{4\pi} \hbar^{-1} \frac{k}{k_o} S(\varkappa, \omega) \qquad (A2)$$

then it is convenient to define R_1 so that:

$$I(\varkappa, \omega) = R_1 \cdot S(\varkappa, \omega) \qquad (A3)$$

In the EA mode one obtains from the treatment of Møller and Nielsen[42], when only the varying part in R_1 is included:

$$R_1 = A_1 \cdot A_2 \frac{A_3}{1+A_3}$$

where

$$A_1 = k^2 \cot\theta_A$$

$$A_2 = k\sigma_{4v} \sqrt{\frac{\sigma_{3v}^2 + 4\eta_A^2 \sin^2\theta_A}{\sigma_{3v}^2 + \sigma_{4v}^2 + 4\eta_A^2 \sin^2\theta_A}} \qquad (A4)$$

$$A_3 = (2\pi)^{5/2} (F_A^3 t_A)/(k^3 \cdot V_A \cdot \eta_A \cdot \sin 2\theta_A \cdot \sin\theta_A)$$

In (A4), A_1 arises from horizontal collimations, A_2 from vertical collimations as calculated in ref. 42, and A_3 is the reflectivity of the analyser

crystal as discussed by Riste[43]. In fig. A2 is shown R_1 calculated for a typical instrumental set up using incident neutron energies of approximately 5, 15, and 40 meV. R_1 was normalized to unity at $\hbar\omega = 0$.

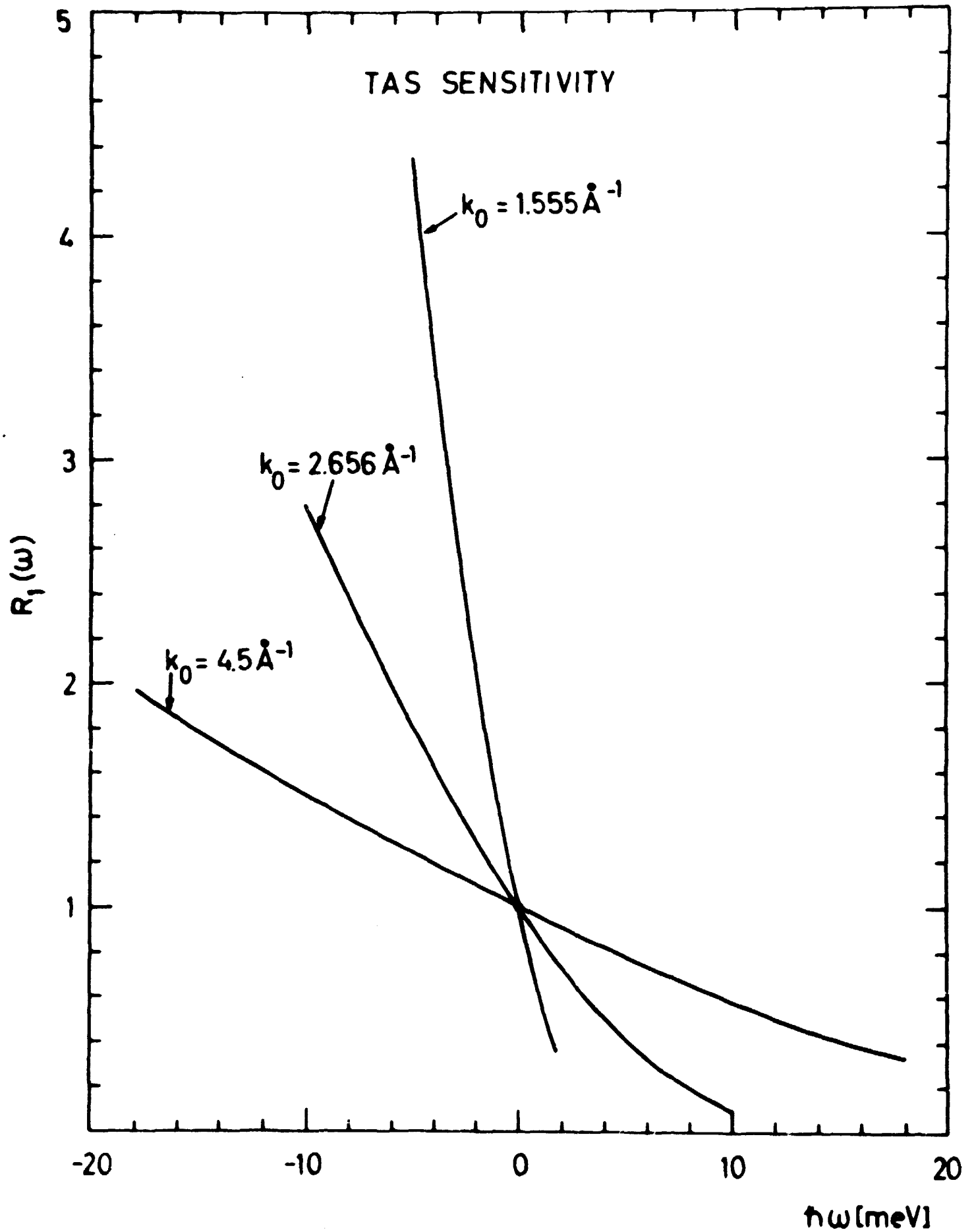

Fig. A2. Intensity corrections for the triple axis spectrometer, shown for a typical set up when operated in the EA mode, discussed in the text.

Considering the large variations of R_1 over a typical energy scan a test of the validity of eq. A4 may be of interest. In fig. A3 the symmetrized coherent scattering law $\tilde{S}_{COH}(\varkappa_o, \omega)$ for liquid N_2 at 66.4 K is shown, obtained by applying eqs. A2, A3, and 13. When 5 meV incoming neutrons

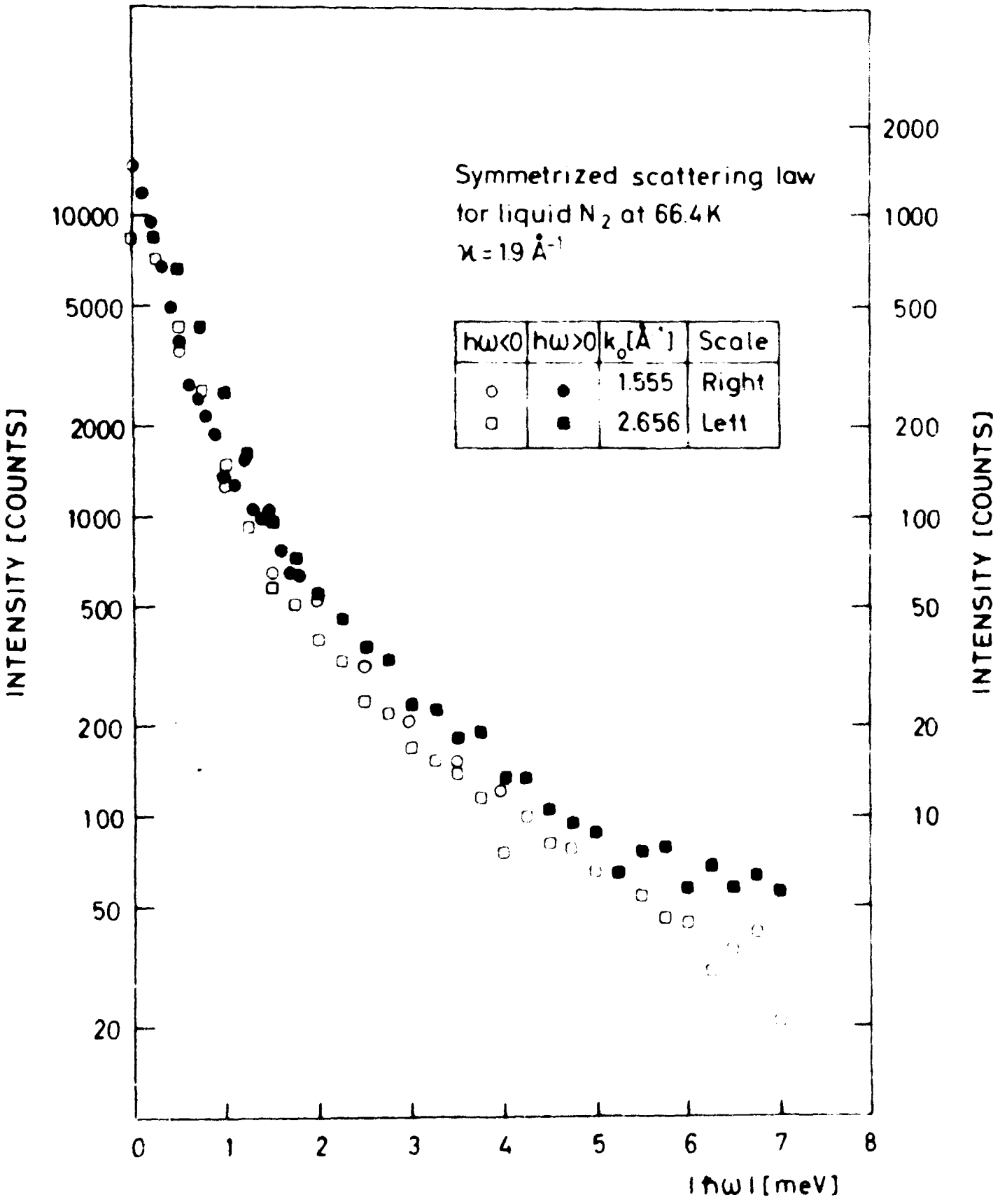

Fig. A3. Symmetrized scattering law for liquid N_2, to test intensity corrections for the triple axis spectrometer.

are used, energy gain and energy loss coincide in fig. A3 showing that $\tilde{S}_{COH}(\kappa, \omega)$ is symmetric, and the difference in the data obtained with 14.7 meV neutrons is probably due to a missetting of the instrument of approximately 0.1 meV. However, the more significant deviation from symmetry seen for energies $|h\omega| > 6$ meV indicates that in this region (13) is no longer valid for the observed scattering. A natural explanation is that multiple scattering dominates in this region. This agrees well with the discussion given in section 4.2.2 and the estimates discussed below.

An alternative and more sensitive test is to measure the scattering from a known system. Here phonons in aluminium were chosen as an example of a harmonic cubic phonon system, and the scans were made in a way insensitive to the only unknown parameter, the Debye-Waller factor. Both focused and defocused scans were performed[42]. The result is shown in fig. A4 so that the dependence on k is shown separately.

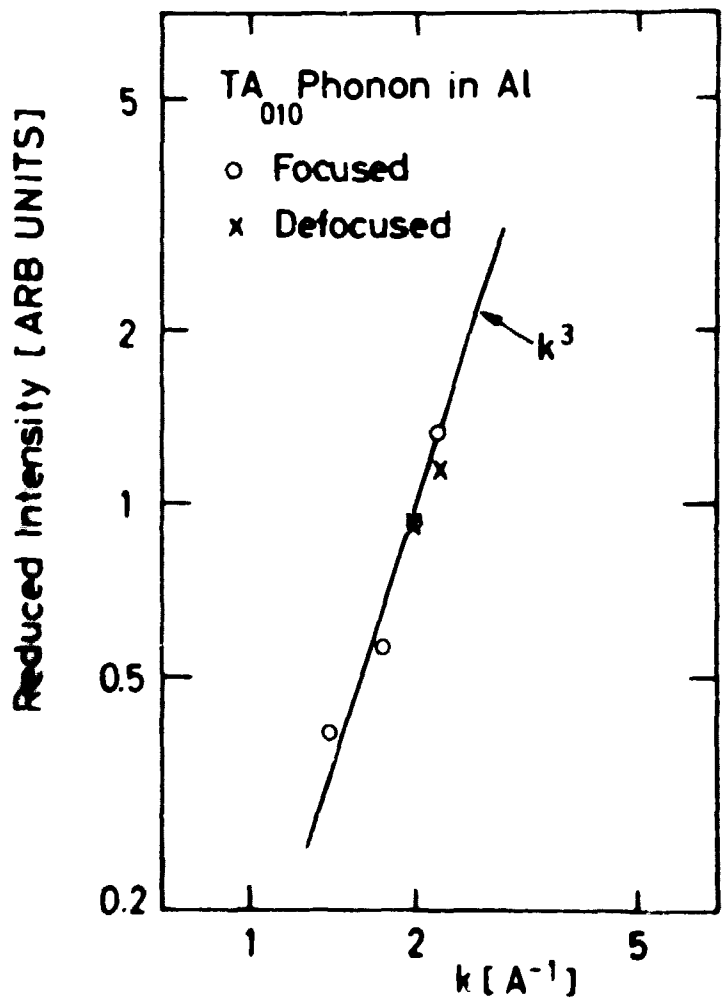

Fig. A4. Intensity of phonons in aluminium, to test the intensity corrections for the triple axis spectrometer. According to the formalism of Møller and Nielsen, the specific k-dependence should be k^3.

The other way of operating the TAS is the FM mode. Here the analyser energy is kept constant, and if one uses a "1/v" monitor before the sample one gets, when the measurement is carried out with the monitor counts constant:

$$R_1 = 1 \qquad (A4)$$

This extremely simple result can, however, only be used in the study of liquids when the incoming energy is so large that third order reflections in the monocromator system can be neglected. Only in this case one can prepare a clean incoming beam using a monocromator crystal with a forbidden second order reflection at the same time as the incoming neutron energy is varied. A test of the validity of eq. A4 shown in fig. 10, where the solid dots correspond to $\hbar\omega < 0$ and open circles to $\hbar\omega > 0$.

A.2.2. The Energy Resolution Function R_2

The influence on the measured spectrum from the form of the resolution function, described by R_2, can in general not be resolved without assuming a certain form for the scattering law under investigation. In liquids, however, one can for lack of a model bypass this problem in two ways.

As mentioned above only the energy resolution is of practical importance in an actual experimental set up, since no strong variation with wavevector is observed. Further since liquid spectra most often show narrow lines only around $\omega \sim 0$ it can be assumed that R_2 is only of importance in this region. In this simplified case one can in principle find the scattering law without assuming any function for the line shape, using the convolution theorem. This procedure was used and discussed by Sköld et al. in the study of liquid A[8].

Considering the numerical problems in performing the actual analysis by the above mentioned method, an alternative method of treating the contribution from energy resolution seemed more attractive. Because R_2 is only of importance in the elastic region of rather small wavevectors, one can investigate this particular region with sufficiently high energy resolution by low energy neutrons, so that the influence of R_2 can be neglected. For intermediate energies where R_2 plays no role in any case, one can then match the results from experiments of low and high incident energies. Such a procedure, easily carried out on a TAS, worked satisfactorily in the case of liquid N_2.

A. 3. Multiple Scattering

In the derivation of absolute scattering laws from neutron scattering results it is essential to correct the data for the contribution from neutrons scattered more than once. At the time where the present experiments were analysed the calculations of Blech and Averbach[44] were the only published prescription of how to analyse this effect. Their results were used to ensure that the multiple scattering was small compared with the primary one, and to choose optimal sample geometries. However, they can only be used as a crude estimate of multiple scattering in inelastic measurements, but as mentioned above, the violation of the principle of detailed balance may be used as an indication that the scattering is no longer dominated by single scattered neutrons. More satisfactory are the recent Monte Carlo simulations of the multiple scattering effect[45].

A. 4. Comparison Between TAS and TOF

On the basis of the neutron scattering results from liquids using either a TAS or a TOF, one cannot in general point towards one as being the best. In favour of the TAS is the flexibility, so that specific constant κ-scans can be performed, and appropriate neutron energies can be chosen to obtain wanted resolution properties. The second order reflections in the crystals do not seem to be a limiting deficiency of this instrument. It might be added that neutron small angle scattering can only be performed on a TAS.

In favour of the TOF in the study of liquids is the better neutron economy since all the neutrons scattered in one direction are simultaneously analysed. This gives automatically the scattering law over a large region of wave-vectors and energies, which is necessary in the study of liquids.

More important than emphasizing a competition between the two types of instruments is probably that the final results agree well independently of which instrument is used. This is shwon in fig. 17 in this report and was also found in ref. 4.